学位論文

Analysis of a mutant collection by chlorophyll fluorescence kinetics

クロロフィル蛍光を用いた遺伝子破壊株コレクションの解析

平成１９年３月博士（生命科学）申請

東京大学大学院新領域創成科学研究科

先端生命科学専攻

尾﨑洋史

CONTENTS

ACKNOWLEDGEMENT

I wish to express my deepest appreciation to Dr. Kintake Sonoike for his constant supervision, advice, discussion and support throughout this study.

I also wish to express my gratitude to Prof. Yoshikazu Ohya for his advice.

I would express my deep appreciation to Hanayo Sato, Hiroyuki Usuki, Banyu Takahashi, Kazumi Shimada, Kazuhiro Hananoi, Mio Tamori for their experimental advice and valuable suggestions. They always support me as members of photosynthesis group.

I am also thankful to Aiko Hirata, Satoru Nogami, Mizuho Sekiya, Machika Watanabe, Yo Kikuchi and Shinichi Onuki for providing a stimulating and supportive environment.

LIST OF TABLES AND FIGURES

Tables

Figures

ABBREVIATIONS

PSII	photosystem II
PSI	photosystem I
PCC	Pasteur culture collection
F	fluorescence
qN	non-photochemical quenching
qP	photochemical quenching
Fm	the maximum level of fluorescence
Fo	the minimal level of fluorescence
Fs	the steady state level of fluorescence
PAM	pulse amplitude modulation
CCD	charge coupled device
OD	optical density
DCMU	3-(3,4-dichlorophenyl-)l,l-dimethylurea
MV	methyl viologen

SUMMARY

The genome sequences of several hundreds model organisms have established a nearly complete list of the genes. The next major challenges are to elucidate the functions of genes in the genome whose functions are currently unknown and to discover how each gene mediates specific biological process.

In chapter I, I describe that the mutants having defect in the regulation of photosystem stoichiometry could be identified through the simple comparison of the induction kinetics of chlorophyll fluorescence of the mutant cells. I made a library containing 500 mutants in the cyanobacterium *Synechocystis* sp. PCC 6803 with transposon mediated gene disruption, and the mutants were served for the measurement of chlorophyll fluorescence kinetics for 45 seconds. I picked up two genes, *pmgA* and *sll1961*, which are involved in the modulation of photosystem stoichiometry. The disruptants of the two genes share the common characteristics in the fluorescence induction kinetics, and I searched for the mutants that showed such characteristics. Out of six mutants identified, five mutants showed different photosystem stoichiometry under high-light condition. The results suggest that the categorization based on the similarity of the fluorescence kinetics could be a novel approach to identify the function of genes.

In chapter II, I established a method to quantitatively analyze chlorophyll fluorescence kinetics. Difference of the "shape" of the two fluorescence kinetics was evaluated as "dissimilarity" that was essentially calculated by the sum of square of deviation at each time point. In addition, several weighting functions were devised to extract the specific characteristics of the mutants having defect in the regulation of photosystem stoichiometry. One of such weighting function, the mutant-specific weighting function is the most objective one, and automatically calculated by focusing on the common characteristics of two fluorescence kinetic data. I screened the mutants for the defect in the regulation of photosystem stoichiometry using the dissimilarity with this mutant-specific weighting function. Nine candidates were listed in addition to the mutants identified in Chapter I. Among them, three mutants were found to have defect in the regulation of photosystem stoichiometry. Thus, the parameter is effective for the *in silico* screening of the mutants at least in the case of photosystem stoichiometry mutants. Furthermore, comparison of the dissimilarity with the profile of gene expression under low- and high-light condition revealed that the dissimilarity could be regarded as a quantitative measure of the phenotype of the mutants. The "shape" of the fluorescence kinetics, the difference of which can be quantified by the dissimilarity parameter, reflects status of cyanobacterial cells and has potential to identify the function of genes.

GENERAL INTRODUCTION

The main target of the biological research in post-genomic era

One of the main goals in post-genomic era is to predict the biological function of each gene on genomes. Many methods have been developed for this purpose, among which the most straightforward way is to apply PSI-BLAST and FASTA to the sequence of the target gene and to find homologs of the gene (Altschul et al. 1997, Pearson, 1998). In this case, the function of the target protein is assumed to be the same with that of its homologs. Generally, this kind of sequence-based method is working well. However, it would not work at all when the sequence similarity between the target protein and known proteins is very low or when the target sequence has homology only to proteins with unknown function. Furthermore, even if the "function" of the target gene could be predicted by these methods, the "role" of the gene in biological system cannot necessarily be revealed. For example, when the gene of interest has homology with a kinase, we can predict the product of the gene would have kinase activity. However, this is not the information we really want to know. We want to know, for example, in which signal transduction pathway the gene is working, or in what kind of biological phenomenon the gene is involved. These pieces of information could not be obtained through the sequence homology.

One of the most powerful techniques to attribute functions to genes in organisms is the analysis of phenotype in gene-disrupted mutants. In this case, "biological phenomenon" could be directly assigned to the gene of interest. However, this approach has also disadvantages in itself. First, it cannot give any information on the function of genes from mutants of which do not exhibit distinguished phenotype. On the other hand, if we employ several kinds of different phenotypes to collect more information, we confront another problem, i.e. how to integrate the different types of information to elucidate the function of the gene. Secondly, although we must first decide what kind of phenotype should be observed in the experiments, it is not easy to find out the suitable method when the function of the genes of interest is totally unknown. Only after we get some information such as, for example, that the gene may be involved in respiration, we could observe the respiration rate as a phenotype. Thirdly, in most cases, phenotype of the mutant must be checked one by one. It is not usually easy to observe the phenotype of the mutants in large scale. Thus, three problems must be cleared for the effective analysis of the mutant phenotype. Requirement 1: The phenotype should be the one that can be observed in high throughput. Simultaneous observation of the phenotype of many mutants should be possible. Requirement 2: We must choose as simple phenotype as possible. The phenotype should be the one that can be treated quantitatively. Nevertheless, the phenotype of as many mutants as possible should be different from that of wild type. Requirement 3: We must choose appropriate phenotype that gives as much information as possible. The phenotype should reflect wide range of cellular processes.

As for the first requirement, several high-throughout biotechnologies have been developed recently. A large number of biological data have been generated, such as yeast two-hybrid systems, protein complex and microarray gene expression profiles and so on. Although these data are rich sources for understanding gene functions, phenotype observation is necessary for the final elucidation of the gene function. Yet another method to analyze gene function is fluorescence measurement technique, which is useful as a non-invasive tool and has extensively been used in biological study. For example, localization of one protein could be predicted by fluorescence of fused green fluorescence protein. In some cases, the condition of the cellular processes can be monitored as a change in fluorescence intensity, or in fluorescence wavelength, or in fluorescence polarization. In the case of photosynthetic organism, they have natural fluorescence probe, chlorophyll, fluorescence of which reflects redox state of photosynthetic electron transfer chain.

Photosynthesis and chlorophyll fluorescence

Oxygenic photosynthesis is the process by which plants, some bacteria and some protists use the light energy to produce carbohydrate from carbon dioxide and water, accompanying evolution of oxygen as a byproduct. Photosynthetic electron transfer is basically conducted on membranes called thylakoid membranes. Although the thylakoid membranes of cyanobacteria are located in cytoplasm, eukaryotic photosynthetic machinery is isolated in chloroplasts enclosed by envelope membranes. The driving force of photosynthetic electron transfer is provided by the two chlorophyll-associated photosystem complexes, photosystem II (PSII) and photosystem I (PSI). The reaction centre of the photosystems is a special pair of chlorophylls, which donates electrons to the initial electron acceptor upon excitation. A pheophytin molecule serves for the electron acceptor in PSII.

The initial electron transfer between the electron donor and electron acceptor is called charge separation. In the case of PSII, negative charge on the initial electron acceptor is subsequently transferred to the secondary electron acceptor Q_A and finally to the terminal electron acceptor Q_B (Renger, 2001). Positive charge on the reaction center chlorophylls is eliminated by electron provided from water splitting machinery in the PSII complexes. Q_B is re-oxidized by plastoquinone in thylakoid membranes that donates electrons to cytochrome b_6/f complexes. From cytochrome b_6/f complexes, electrons go to PSI via plastocyanin or cytochrome c_6 (Hope, 1993). Another charge separation induced in PSI transfers electrons to $NADP^+$ via ferredoxin (Hervas et al. 2003), thus producing NADPH that is used for the reduction of carbon dioxide to carbohydrate. The electron transfer through the two photosystems not only provide reducing power for the fixation of carbon dioxide but also provide ATP through the formation of proton gradient across the thylakoid membranes. Electrochemical potential of the proton gradient drives the proton flux through

ATP synthase that is also embedded in thylakoid membranes.

Under normal condition, the light energy absorbed by chlorophylls are mainly used for driving the above mentioned electron transfer. Thus, only a small fraction (2-8%) of the energy is re-emitted as fluorescence in photosynthetic apparatus (Latimer et al. 1956, Trissl et al. 1993). However, the quantum yield of fluorescence of chlorophyll solution in organic solvents (where excitation energy transfer and photochemistry do not occur) is about 20-35% (Latimer et al. 1956). The chlorophyll fluorescence characteristics is also different between PSI and PSII. At room temperature, quantum yield of fluorescence from PSII is much higher than that from PSI (Paillotin, 1976, Krause and Weis, 1991). Accordingly, the chlorophyll fluorescence from photosynthetic machinery at room temperature mainly reflects the condition of PSII.

Light energy absorbed by chlorophyll molecules in vivo can be directed to one of three fates: it can be used to drive photosynthesis, excess energy can be dissipated as heat or it can be re-emitted as chlorophyll fluorescence. These three processes occur in competition, such that any increase in the efficiency of one will result in a decrease in the yield of the other two. Hence, by measuring the yield of chlorophyll fluorescence, information on the changes in the efficiency of photochemistry and heat dissipation can be obtained. Thus, chlorophyll can be regarded as an intrinsic fluorescent probe of the photosynthetic systems. The yield of chlorophyll fluorescence depends, in a large part, on the capacity of photosystem II to carry out a stable charge separation between a special chlorophyll pair and Q_A, the primary quinone acceptor of the reaction center (Lazar, 1999). When Q_A is oxidized, the reaction center is able to utilize the light energy for charge separation, leading to the low yield of chlorophyll fluorescence. In contrast, when Q_A is reduced, the reaction center is unable to undergo stable charge separation and the yield of chlorophyll fluorescence becomes high.

Changes in the yield of chlorophyll fluorescence were first observed by Kautsky and Hirsch. They found that, when dark-adapted photosynthetic organisms are illuminated with continuous light, chlorophyll fluorescence displays characteristic changes in intensity accompanying the induction of photosynthetic activity. The change in the intensity of chlorophyll fluorescence is usually called induction kinetics of chlorophyll fluorescence. When a dark-adapted plant is exposed to continuous light, initial increase in the yield of chlorophyll fluorescence occur that reflects reduction of Q_A. Following the increase, the fluorescence level typically starts to fall again. This reflects the activation of enzymes involved in the downstream of electron transfer leading to the partial re-oxidation of Q_A. There are several steps in photosynthetic electron transfer that could be light-activated: ferredoxin-NADPH oxidoreductase (FNR) or several enzymes in Calvin cycle (Buchanan and Luan, 2005). The activation time course of these enzymes affects the induction kinetics of the chlorophyll

fluorescence. Furthermore, proton gradient formed by the electron transfer suppresses the rate of electron transfer itself. This feed-back regulation also affects the induction kinetics. Thus, the intensity of chlorophyll fluorescence from photosynthetic apparatus shows very complex changes reflecting the condition of many components of photosynthetic metabolism.

Cyanobacteria as model organisms for photosynthetic study

During the evolution of the modern biosphere, photosynthetic processes in cyanobacteria have played a central role by elevating the oxygen level in the atmosphere of the Earth that starts 2.7 billion years ago. Compared with other eubacteria, a unique feature of cyanobacteria, the largest group of oxygenic photosynthetic prokaryotic organisms, is the presence of a differentiated membrane system. Similar to other Gram-negative bacteria, cyanobacteria have an envelope layer consisting of an outer membrane, a peptidoglycan layer, and a plasma membrane. In addition, these organisms have a distinct intracellular membrane system, the thylakoids, which are the sites for both oxygenic photosynthesis and respiration (Gantt, 1994). Cyanobacteria are the progenitors of chloroplasts in green plants so that the basic machinery of photosynthesis in cyanobacteria is the same as that of plants. From the photosynthetic point of view, cyanobacteria are different from the photosynthetic bacteria such as green sulfur bacteria or purple bacteria, and more similar to algae and higher plants. As a prokaryote, cyanobacteria has simple cell structure without organelle, and homogeneous cell culture can be prepared for both physiological and biochemical study. Thus, cyanobacteria are widely used for the study of photosynthesis. Among several cyanobacterial strains, the unicellular, naturally transformable cyanobacterium *Synechocystis* sp. PCC 6803 is the first photosynthetic organism with a completely sequenced genome (Kaneko et al. 1996). This organism offers an excellent experimental system to investigate the photosynthetic apparatus, especially when the molecular biological approach is taken.

Strategy to approach function of genes

As stated above, three requirements are necessary for the elucidation of the gene function: 1) high throughput phenotype analysis, 2) simple and quantitative phenotype, and 3) phenotype that reflects wide range of cellular processes. Here I employ chlorophyll fluorescence as a phenotype to analyze the gene function because of the following reasons. First, chlorophyll fluorescence is easily monitored by optical devises, and simultaneous measurements of many mutants are possible for high throughput analysis. Secondly, induction kinetics of the chlorophyll fluorescence could be expressed as simple one-dimensional numerical figures that are easy to handle. Finally, chlorophyll fluorescence reflects the condition of photosynthetic electron transport. In plant cell, photosynthesis is conducted in chloroplasts, and consequently, chlorophyll

fluorescence principally reflects the condition of photosynthesis. In cyanobacteria, however, photosynthetic and other metabolic pathways are not separated in organelles. Thus, chlorophyll fluorescence of cyanobacteria possesses a potential to detect the effects of mutation not only on photosynthesis but also on the wide variety of metabolic systems. If a broad range of effects from mutation is detected by one phenotype, many kinds of mutants are characterized simply by the phenotype. In this study, I focused on induction kinetics of chlorophyll fluorescence emitted from cyanobacteria and explore the possibility to obtain information on the function of wide range of genes.

CHAPTER I

Investigation of chlorophyll fluorescence kinetics to identify the factors involved in the modulation of photosystem stoichiometry

INTRODUCTION

The complete sequences of nearly 300 genomes have become available, with another 750 projects underway. Although sequence information of genomes provides the foundation to analyze genes on the genomes, the sequence information itself is not sufficient to reveal the function of each gene. For that purpose, phenotype analysis of mutants is indispensable. The large-scale analysis of the mutant libraries should potentially facilitate the comprehensive identification of function of genes in a wide range of biological processes. Generating mutant libraries through random whole-genome transposon-insertion mutagenesis followed by sequence-based identification of insertion sites has been widely used for a wide variety of microbes such as *Neisseria meningitidis* (Geoffroy et al. 2003), *Mycoplasma* (Hutchison et al. 1999), *Pseudomonas aeruginosa* (Jacobs et al. 2003), *Helicobacter pylori* (Salama et al. 2004), and *Saccharomyces cerevisiae* (Scherens and Goffeau, 2004). Screening of the mutant libraries allows the characterization of many known and unknown genes by looking at the phenotypes such as sporulation (Ross-Macdonald et al. 1999), growth in high-salt medium (de Jesus Ferreira et al. 2001) or ethanol tolerance (Takahashi et al. 2001).

For plants and other photosynthetic organisms, chlorophyll fluorescence has been often used for screening. The yield of chlorophyll fluorescence from photosynthetic organisms that have been dark-adapted for some time shows complex kinetic changes upon actinic illumination. This kinetics of chlorophyll fluorescence is called "Kautsky effect", which reflects the change in the condition of photosynthesis that is the most important metabolic pathway in plants (Govindjee, 1995). Use of chlorophyll fluorescence is advantageous for the large-scale screening, since it can be easily monitored non-destructively using charge coupled device (CCD) camera. For example, the mutants with defects in xanthophyll-cycle activity were isolated by the analysis of digital video image of chlorophyll fluorescence in *Chlamydomonas reinhardtii* (Niyogi et al. 1997) or in *Arabidopsis thaliana* (Niyogi et al. 1998, Li et al. 2000). Similar imaging of chlorophyll fluorescence was used for the isolation of mutants with modified activity of NAD(P)H dehydrogenase in *A. thaliana* (Hashimoto et al. 2003, Munshi et al. 2005, Munshi et al. 2006). In the former case, non-photochemical quenching of chlorophyll fluorescence was used for the measure of the activity of xanthophyll cycle. In the latter, transient increase in the chlorophyll fluorescence after turning off of the actinic light was used for the criterion for the activity of NAD(P)H dehydrogenase. Although these methods enable us to search for mutants that have defects in the specific

function, they could not be applied to the screening of the mutants whose phenotype is not clearly established.

I propose a new type of screening in this study. The method is simply based on the similarity of fluorescence kinetics among the mutants and does not require the theoretical relationship between the kinetics of fluorescence and physiological condition of the mutants. The idea came from the analysis of the mutants that have defect in the modulation of photosystem stoichiomtery. Since PSII and PSI function in tandem during photosynthetic electron flow, photosynthetic organisms must maintain a balance of the two photosystems. For example, changes in the light quantity induce the modulation of PSI/PSII ratio in cyanobacteria (Fujita, 1997). PSI/PSII ratio decreases in cyanobacteria upon the shift to high light condition through the selective suppression in the amount of PSI, in addition to the general decrease in the amount of both photosystems. The role of the regulation of photosystem stoichiometry during acclimation to high light is apparently not to maintain optimal photosynthesis but to protect the cells from oxidative damage through the suppression of photosynthetic electron transfer (Sonoike et al. 2001). The disruption of genes involved in the transcription, translation, assembly, or biogenesis of PSI or PSII may be involved in the regulation of photosystem stoichiometry. However, only a few mutants that have defect in the regulation of photosystem stoichiometry under high-light conditions has been reported so far. Recently, several mutants of the cyanobacterium *Synechocystis* sp. PCC 6803 were isolated that showed different induction kinetics of chlorophyll fluorescence from that of the wild type. Among the mutants, *sll1961* mutant exhibited fluorescence kinetics similar to *pmgA* mutant that had been reported to have a defect in the regulation of photosystem stoichiometry (Fujimori et al. 2005). Indeed, the detailed characterization of *sll1961* mutant revealed that this mutant could not regulate photosystem stoichiometry (Fujimori et al. 2005). Thus, the results open a way for the method to identify the mutant with defect in the regulation of photosystem stoichiometry by simply monitoring the kinetics of chlorophyll fluorescence. In this study, I made a library of cyanobacterial mutants with transposon-mediated mutagenesis, and screen for the library with the similarity of the fluorescence kinetics with each other. The results clearly indicated the practical effectiveness of the method focusing on the fluorescence kinetics pattern to identify the mutant with modified photosystem stoichiometry.

MATERIALS AND METHODS

In vitro transposon mutagenesis and sequence analysis

Transposon mutagenesis on cosmid clones containing *Synechocystis* sp. PCC 6803 genome fragment (Kaneko et al. 1996) was carried out using the pGPS-1 plasmid and the GPS-1 genome priming system (New England Biolabs, USA) according to the manufacturer's protocol. Mutagenized cosmid DNA was introduced to *E. coli* and transformants were plated onto selective media

containing ampicillin (50 μg/ml) and chloramphenicol (20 μg/ml). The mutated cosmids were recovered from the transformed *E. coli* cells and the site of the transposon insertion was identified by direct sequencing with the primer 5'-CACAGCATAACTGGACTGATTTCAG.

Strains and growth conditions

A glucose-tolerant wild-type strain *Synechocystis* sp. PCC 6803 was grown in BG-11 medium (Rippka et al. 1979) buffered with 10 mM N-tris(hydroxymethyl)methyl-2-aminoethanesulfonic acid (TES)-NaOH (pH 8.0). Cells were grown under continuous illumination at 30°C. Liquid cultures were bubbled with air. Solid medium was supplemented with 1.5% (w/v) agar and 0.3% (w/v) sodiumthiosulfate. To support photomixotrophic growth, glucose was added to a concentration of 5 mM. Photon flux density at 20, 100 and 200 μmol photons m^{-2} s^{-1} was regarded as low, medium and high light, respectively. For creating site directed mutants, the wild-type strain was transformed by the mutated cosmid described above, and chloramphenicol-resistant clones were selected on solid media. Resistant colonies were serially re-streaked at least five times on BG-11 agar plates supplemented with antibiotics (8.0 μg of chloramphenicol/ml) to promote the segregation of the mutant genome. The *pmgA* (*sll1968*) mutant was created by insertion of the spectinomycin resistant cassette (Hihara and Ikeuchi, 1997). The *sll1961* mutant was generated by the insertion of a transposon that has a chloramphenicol-resistant cassette (Fujimori et al. 2005). Site-directed mutants and *sll1961* mutant were maintained with 8 μg/ml chloramphenicol, while the *pmgA* mutant was maintained with 20 μg/ml spectinomycin.

Monitoring of chlorophyll fluorescence kinetics

10 μl of cell culture, of which OD_{730} was adjusted to 0.5 by BG-11 liquid medium, was dropped on BG-11 agar plates. The wild type cells of 1.1 x 10^8 cells ml^{-1} showed 1 OD_{730}, when OD was determined by a spectrophotometer (GeneSpec III, Hitachi, Japan). After incubation at 30°C under the light at 20 μmol m^{-2} s^{-1} for 72 h or at 200 μmol m^{-2} s^{-1} for 48 h, the plates were subjected to the measurements of chlorophyll fluorescence kinetics. Cells on agar plates were dark adapted for 15 min before the measurements. The plates were put in fluorescence imaging system (FluorCam 700MF, Photon System Instruments, Czech Republic) and actinic light (200 μmol m^{-2} s^{-1}) was applied for 45 s to monitor chlorophyll fluorescence. The actinic light was generated by two panels of orange light-emitting diodes (HLMP EH08, Agilent Technologies, USA) with peak wavelength at 615 nm and the spectral half-width of 18 nm. Fluorescence image was captured every 0.04 s for 45 s by a CCD camera (ICX429AL, Sony, Japan) that produced 752 x 580 pixel images in an 12 bit gray scale. The sensitivity was adjusted to 20% on the FluorCam software. The fluorescence around 700 nm was detected by filtering the emission through

a custom-made interference filter with a peak at 700 nm (the full-width at half-maximum is 30 nm) and a red blocking filter (RG697, Corion, USA). The fluorescence intensity was normalized with initial value at the start of actinic light.

Absorption spectra of cell suspensions at room temperature

In vivo absorption spectra of whole cells of the wild type and mutants suspended in BG-11 medium were measured at room temperature using a spectrophotometer (Model 356; Hitachi, Japan) with a cuvette placed just in front of a photomultiplier to minimize the effect of scattering on absorption spectra. Concentration of chlorophyll was calculated by the equations of Arnon et al. (1974). Chlorophyll content of cells was normalized at OD_{730} determined by a spectrophotometer (Model 356; Hitachi, Japan) with a cuvette placed just in front of a photomultiplier. The wild type cells of 3.3×10^{10} cells ml^{-1} showed 1 OD_{730}, when OD was determined under this condition. I microscopically determined cell numbers of the wild type strain using a Neubauer improved haemocytometer.

Fluorescence emission spectra determined at liquid nitrogen temperature

Low temperature fluorescence emission spectra at liquid nitrogen temperature (77 K) were recorded using a custom-made apparatus (Sonoike and Terashima, 1994). Cell suspensions at a chlorophyll concentration of 5 μg chlorophyll ml^{-1} in BG-11 medium were injected into brazen sample holders and frozen by immersing them into liquid nitrogen. The cell suspensions were excited by blue light passing through a broad band-pass filter (CS 4-96, Corning Inc., USA). Before the measurement, cells were incubated in darkness for 10 min at room temperature to equilibrate the redox state in photosynthetic electron transfer chain. Under this condition, the intensity ratio of PSI fluorescence at 725 nm and PSII fluorescence at 695 nm gives infomation on the relative raito of photosystem contents.

Analysis of Chlorophyll Fluorescence by PAM fluorometer

Chlorophyll fluorescence was measured with a pulse-amplitude modulation chlorophyll fluorometer (PAM 101/102/103, Heinz Waltz, Germany) with a high sensitivity emitter-detector unit (ED-101US, Heinz Waltz, Germany) as described by Sonoike *et al.* (2001). Cells were dark-adapted for 5 min, and then the measuring light was turned on to obtain the minimal fluorescence level (*Fo*). The steady state level of fluorescence (*Fs*) was determined during the exposure of cells to actinic light from a light source (KL 1500, Wiesbaden, Germany) with defined photon flux density. The fluorescence level with fully reduced Q_A (*Fm'*) was obtained by applying multiple turnover flashes (XMT 103, Heinz Waltz, Germany) under actinic light. The far-red light from a photodiode (FR 102, Heinz Waltz, Germany) was applied just after turning off

the actinic light to obtain quenched level of Fo (*Fo'*). The maximum fluorescence (*Fm*) was obtained by adding 10 μM DCMU to the sample under actinic light. Photochemical quenching (qP) and non-photochemical quenching (qN) were calculated as (*Fm'* - *Fs*)/(*Fm'* - *Fo'*) and 1 - [(*Fm'* - *Fo'*)/(*Fm* - *Fo*)], respectively.

RESULTS

Construction of Synechocystis mutant library

106 cosmid clones used for the whole genome sequencing of *Synechocystis* sp. PCC 6803 (Kaneko et al. 1996), which covers 89% of the ORFs in the genome, was used for the mutagenesis. The each cosmid clone was mutagenized in vitro with transposon and transformed into *Escherichia coli* cells to pick up individual mutated cosmid clones. By sequencing the border regions between transposon and *Synechocystis* genomic DNA using transposon-specific DNA primer, 1092 cosmid clones with disruption at different ORFs were selected. Then, they were used for generating insertional mutant of *Synechocystis* by homologous recombination. I generated 500 mutants that extended across all the gene categories at 1st level in CyanoBase (http://www.kazusa.or.jp/cyano/) (Table 1-1). The coverage of ORFs is lowest in the category "Cell envelope" (7.5%) and highest in the category "Energy metabolism" (25.8%). The total coverage of this library is about 15% of the genome.

Isolation of the mutants with similar chlorophyll fluorescence induction kinetics to pmgA and sll1961 mutants

I first grow the cyanobacteria in patches with a diameter of about 1 cm on plates under low-light (20 μmol m^{-2} s^{-1}) or high-light (200 μmol m^{-2} s^{-1}) condition, and then the plates were dark adapted for 15 minutes and subjected to the fluorescence measurements. Two-dimensional fluorescence images were collected in every 40 ms for 45 seconds starting at the onset of the orange actinic light (Fig. 1-1). The intensities of the fluorescence from each patch of cyanobacteria in each image were integrated, and the resulting one-dimensional data (i.e. fluorescence kinetics) were used for the detailed analysis of the influence of the gene disruption in each mutant. Examination of the fluorescence kinetics of *sll1961* mutant (Fig. 1-2B (1)) and that of *pmgA* mutant (Fig. 1-2B (2)) revealed that both mutants showed lower first peak (at around 0.5 second after the onset of the illumination) than that of the wild type (Fig. 1-2B) under high-light condition but the kinetics were more or less similar under low-light condition (Fig. 1-2A (1), (2)), which is consistent with earlier report (Fujimori et al. 2005). In addition, the final level of the fluorescence (at 45 second after the onset of the illumination) is higher than the initial peak in the mutants but not in the wild type only under high-light condition. Next, I systematically determined the fluorescence kinetics of the transposon-inserted mutants and sought for the

mutants that shared similar characteristics of the fluorescence kinetics with the *sll1961* and *pmgA* mutants. Among 500 mutants, six mutants showed fluorescence kinetics similar to the *sll1961* and *pmgA* mutants under high-light condition (Fig. 1-2B 3-8). Under low-light condition, all the six mutants showed similar fluorescence kinetics to the wild type with one exception: the mutant of *slr0249* showed more pronounced difference under low-light condition than under high-light condition. Annotations of the genes that disrupted in the mutant were summarized in Table 1-2.

Characteristics of photosynthetic apparatus of the isolated mutants

Fluorescence emission spectra of the mutant and the wild type strains were determined at liquid nitrogen temperature in order to detect possible differences in photosystem stoichiometry between them. The fluorescence at 725 nm is predominantly emitted from PSI while that at 695 nm arises mainly from PSII at low temperature (Fig. 1-3). Thus, the ratio of fluorescence intensity at 725 nm and that at 695 nm determined at 77 K (F_{725}/F_{695}) is a good indicator of PSI/PSII ratio. Figure 1-4A shows the relative fluorescence intensity of the cells grown in liquid culture under low-light or high-light condition. Cells of *ctaEI*, *ctaCI*, *ccmK2*, *slr1916* and *slr0645* mutant strains grown under low light exhibited no significant difference in PSI/PSII ratio compared with wild-type cells. Under high-light condition, however, they showed a higher level of PSI/PSII compared with the wild type cells. These characteristics is quite similar to that observed for *pmgA* and *sll1961* mutants. The results indicate that photosystem stoichiometry of the five mutants is different from that of wild type only under high-light condition. In the case of *slr0249* mutant, the PSI/PSII ratio was lower than the wild type under low-light condition and similar to the wild type under high-light condition.

Increase of F_{725}/F_{695} could be caused either by the increased level of PSI or by the decreased level of PSII. It is expected that higher PSI level would result in higher chlorophyll content, since nearly 90% of the chlorophyll molecules are associated with PSI in cyanobacteria. The chlorophyll content would not be much affected by the change in the level of PSII, in which main antenna pigments are not chlorophyll but phycobiliproteins. Absorption spectra of whole cells of the wild type and the mutants suspended in BG-11 media were measured to estimate chlorophyll contents per cell basis. The four mutants (*sll1961*, *pmgA*, *ccmK2* and *slr1916*) showed higher chlorophyll level than the wild type in the cells grown under high light and possibly in the cells grown under low light (Fig. 1-4 (C), (D)). On the other hand, the three mutants (*ctaEI*, *ctaCI* and *slr0645*) did not show the increased level of chlorophyll content compared with the wild type both in the cells grown under high-light condition and low-light condition. These results suggest that the cause of the high F_{725}/F_{695} ratio in the high-light grown cells of *sll1961*, *pmgA*, *ccmK2* and *slr1916* mutants is increase in PSI content compared with the wild type. On the other hand, *ctaEI*,

ctaCI and *slr0645* mutants grown under high-light condition would have a decreased level of PSII. In the case of *slr0249* mutant, there observed a decrease of F_{725}/F_{695} compared with wild type under low-light condition and a small decrease of chlorophyll compared with wild type under high-light condition. Since the growth of this mutant is rather slow both under high-light and low-light condition (see below), it is difficult to discuss on the cause of the change in photosystem stoichiometry under the possible secondary influence from the slow-growth.

The six mutants were thus divided into three groups according to two parameters, F_{725}/F_{695} and the level of chlorophyll. Group I, consisting of *sll1961*, *pmgA*, *ccmK2* and *slr1916* mutants, showed high value of both parameters under high-light condition (Fig. 1-4D, solid circle) but the phenotype was weaker under low-light condition (Fig. 1-4C). Group II, consisting of *ctaEI*, *ctaCI* and *slr0645* mutants, showed high value of F_{725}/F_{695} but normal value of chlorophyll content under high-light condition (Fig. 1-4D, broken circle). The phenotype of the Group II mutants disappeared almost entirely under low-light condition (Fig. 1-4C). Group III consists of only *slr0249* mutant (Fig. 1-4D, square). Group III showed lower value of F_{725}/F_{695} under low-light condition and lower value of chlorophyll concentration under high-light condition compared with the wild type (Fig. 1-4C and D).

Monitoring of photosynthetic characteristics by PAM fluorometer

Modified amount of photosystems would lead to the altered photosynthetic characteristics. I determined the photosynthetic characteristics of the wild type and the mutants grown under low and high light conditions for 24 h using PAM fluorometer. The quantified values (Fv/Fm: maximum quantum yield of PSII, NPQ: a parameter reflects any process other than photochemistry which lowers the yield of variable fluorescence, qP: an indicator of the redox state of plastoquinone pool, ϕII: quantum yield of electron transfer through PSII) from the fluorescence measurements were shown in Table 1-3. In high light acclimated *slr0249* mutant cells, no significant differences from the wild type were observed. In cells of low light acclimated *slr0249* mutant, however, Fv/Fm, qP and ϕII were lower than that in the wild type, although there was no significant difference in NPQ. *slr0249* mutant would have a defect on PSII. In low light acclimated cells of *ccmK2* and *slr1916* mutants, the two mutants were not significantly different from the wild type in any photosynthetic parameters. On the other hand, high light acclimated cell of *sll1961, pmgA, ccmK2* and *slr1916* mutants showed low Fv/Fm and NPQ. In the case of *ctaCI, CtaEI* and *slr0645* mutants, significant difference was not detected by PAM fluorometer either in low light acclimated cells or in high light acclimated cells.

Growth under photomixotrophic condition

It was reported that growth of *pmgA* mutant is severely suppressed

under photomixotrophic conditions with 5 mM glucose and the medium light at 50 μmol m^{-2} s^{-1} (Hihara and Ikeuchi, 1997). All the mutants and the wild type could grow on the BG-11 agar plate containing 5 mM mannitol, a nonpermeable solute, under photon flux density at 100 μmol m^{-2} s^{-1} (Fig. 1-5, lower part). In the presence of 5 mM glucose, the growth of the entire Group I mutants (*pmgA*, *slr1961*, *ccmK2* and *slr1916*) were severely suppressed while that of Group II mutants (*ctaEI*, *ctaCI*, *slr0645*) were the same with that of the wild type (Fig. 3, upper part). The growth of *slr0249* mutant was always slower than that of the wild type irrespective of the growth condition.

DISCUSSION

Fluorescence kinetics as a tool to analyze phenotype of mutants

Here we demonstrate that the simple monitoring of chlorophyll fluorescence could be used to screen the mutants with the defect in the regulation of photosystem stoichiometry. Out of six candidates that showed similar fluorescence kinetics to that of two known mutants of *sll1961* and *pmgA*, five mutants (*ccmK2*, *slr1916*, *ctaEI*, *ctaCI*, *slr0645*) showed defect in the regulation of photosystem stoichiometry under high-light condition. The rest one (*slr0249*) showed the abnormal photosystem stoichiometry only under low light condition, which may be due to the slow growth of this mutant. In any event, the characteristic change of fluorescence kinetics in the mutants is efficient and convenient way to find the regulatory component of photosystem stoichiometry.

It should be noted that the method presented here does not assume any theoretical relationship between fluorescence kinetics and the physiological consequences of the modified photosystem stoichiometry. Since the discovery of "Kautsky effect" of the chlorophyll fluorescence, the complex kinetics of the fluorescence has attracted the interest of many people and interpretation of the "meaning" of the kinetics was always the point at issue (Govindjee, 1995, Lazar, 1999). In this study, however, the similarity of the "shape" of the fluorescence kinetics is the only criterion to screen the mutants. Thus, there is a possibility that this method could be applied to the screening for any other regulatory components of photosynthesis. Moreover, it may be even possible to apply to the screening the factors that is not directly related to photosynthesis when we use cyanobacteria as an experimental material. In plant cell, photosynthesis is conducted in chloroplasts, and consequently, chlorophyll fluorescence principally reflects the condition of photosynthesis. In cyanobacteria, however, photosynthetic and other metabolic pathways are not separated in organelles. Respiratory electron transport chain shares several components with photosynthetic electron transport chain, and carbohydrate metabolism and nitrogen metabolism have relation with photosynthesis through the production and consumption of ATP or reducing power (Scherer et al. 1988, Hart et al. 2005, Flores et al. 2005). It has been established that all the metabolic pathways are related with each other on metabolic network, and local perturbations in

metabolite concentrations could reach the whole network (Barabasi and Oltvia 2004). Chlorophyll fluorescence from cyanobacteria would reflect the condition of not only photosynthesis but also a wide variety of metabolic systems and cellular processes because photosynthesis in cyanobacteria is a part of metabolic networks in a same compartment. Thus, the method developed in the present study possesses a possibility to investigate various networks including photosynthesis. The fluorescence kinetics of the mutants could be easily registered in a database, since the data themselves are simple one-dimensional array of rational numbers. One can search for the fluorescence kinetics in the database based on the similarity to the kinetics observed in the mutant of interest. In such a way, candidates for the factors that are involved in the interested process could be easily listed. Such possibility should be examined in near future.

In this study, 500 mutants of *Synechocystis* PCC 6803 were created. Since cyanobacteria usually have about 10 copies of genomes in a cell, it is necessary to use a process to promote segregation of the genome to obtain fully segregated mutants. The procedure to promote segregation employed in this study (re-streaking of cells on plates containing antibiotics for 5 times) does not necessarily guarantee the full segregation of the genomes. There are losses and gains on this point. The phenotypes of the mutants may not be stable because of the possible change in the levels of segregation. On the other hand, the procedure enables to collect the information on the mutants of essential genes of which we could not obtain segregated mutants. Since I aimed high-throughput screening of the mutant, I judged that the strategy to use latter advantage is more appropriate for my purpose. The genome-wide collections of the mutants have been shown to be useful for the analysis of gene function in many organisms but there was no such collection in *Synechocystis* PCC 6803. The collection of the cyanobacterial mutants I created in this study would be useful for the research community of photosynthesis as well as of cyanobacteria.

The factors involved in the regulation of photosystem stoichiometry

The regulation of photosystem stoichiometry as a response to the changes in light environments has been widely observed in cyanobacteria (Kawamura et al. 1979, Fujita et al. 1985, Manodori and Melis 1986, Hihara et al. 1998), algae (Melis et al. 1996) and higher plants (Chow et al. 1990). The dynamic alteration in the composition of thylakoid membranes is brought about in order to optimize the excitation of the two photosystems under different qualities of light (Fujita 1997), or to protect the cells from photodamage under high photon flux densities (Hihara et al. 1998, Sonoike et al. 2001). It is also reported that the stoichiometry is modulated by nutrient availability or affected by mutations of several genes (Melis et al. 1985). Evidences from characterization of the mutants defective in the regulation of the photosystem stoichiometry suggested that the modulation of photosystem stoichiometry in

cyanobacteria is an essential response to long-term high-light condition (Hihara et al., 1998, Fujimori et al. 2005). Only two regulatory mutants of photosystem stoichiometry under high light condition have been reported so far, although the physiological aspects of the regulation of photosystem stoichiometry have been extensively studied. In this study, six other candidates for the regulatory component of photosystem stoichiometry were found. Among them, two mutants (*ccmK2* and *slr1916* mutants), together with *sll1961* and *pmgA* mutants, clearly categorized in one group (Group I) with two criteria: 1) increased PSI content under high light condition and 2) impairment in the growth under photomixotrophic condition. Gene product of *ccmK2* is a shell protein of carboxysomes (Cannon et al. 2002). At first glance, the inability of the regulation of photosystem stoichiometry does not seem to be directly related to the disruption of *ccmK2* gene. However, I could exclude the possibility of secondary mutation on *sll1961* and *pmgA* genes in *ccmK2* and *slr1916* mutants by sequencing of coding regions of *sll1961* and *pmgA* genes in the mutants. One explanation for the finding is the indirect effect of the carbon concentrating mechanisms on the photosystem stoichiometry through the change in cellular CO_2 concentration. High PSI/PSII ratio was observed in *Anacystis nidulans* cells under low CO_2 condition and this relative increase of PSI in low-CO_2 grown cells was explained as to meet the demand to generate extra ATP through cyclic electron transfer, which is necessary to import inorganic carbon (Manodori and Melis 1984). High light condition increases demand for inorganic carbon and *ccmK2* mutant would have less activity of inorganic carbon uptake than the wild type. The increased amount of PSI in *ccmK2* mutant grown under high light condition might be a result of increased demand for CO_2. *slr1916* has esterase domain but its function is unknown. These genes may affect photosystem stoichiometry through the change in photosynthetic or other metabolic pathways. It was reported that the mutant of *pmgA* could not grow under photomixotrophic growth condition, although the mechanism of the photomixotroph-sensitivity in the mutants is totally unknown (Hihara and Ikeuchi, 1997). It is clear that the growth of the mutants of Group I genes (*pmgA*, *sll1961*, *ccmK2* and *slr1916*) were all severely suppressed under photomixotrophic condition (Fig. 1-5). Defect in the decrease of PSI content under high-light condition must be related to the growth sensitivity under photomixotrophic condition but the actual mechanism of this sensitivity is currently unknown.

Group II mutants seem to have lower PSII content under high-light condition. Among them, I found two mutants that have defect in cytochrome *c* oxidase. Cytochrome *c* oxidase, composed of the three subunits CtaC, CtaD and CtaE, is a component of the respiratory chain that catalyzes the reduction of oxygen to water and generates an electrochemical potential that can provide energy for numerous cellular processes. It was reported that over-reduction of PQ pool presumably take place in thylakoid membranes of the cytochrome *c* oxidase mutant (Kufryk and Vermaas. 2006). In addition, cytochrome *c* oxidase

mutants were reported to exhibit decreased level of PSII with little loss of chlorophyll content (Nomura et al. 2006). Close look at the chlorophyll fluorescence kinetics in the *ctaEI* and *ctaCI* mutants (Fig. 1-2) revealed the transient decrease of chlorophyll fluorescence intensity at 40 ms and 80 ms after onset of the actinic light. The decrease seemed to be explained by the oxidation of the plastoquinone pool that had been reduced in the dark in the absence of cytochrome *c* oxidase. Cytochrome *c* oxidase is the major terminal accepter for electrons from the plastoquinone pool in the dark while PSI should be the primary electron acceptor from the plastoquinone pool in the light. Observed change in the photosystem stoichiometry could be the result of reduced plastoquinone pool in the mutants. Another mutant in Group II is *slr0645* mutant. *slr0645* encodes hypothetical protein with a von Willebrand factor type A (vWA) domain. Since this domain is supposed to serve for the protein-protein interaction, regulation of photosystem stoichiometry through such interaction with other component(s) may be possible.

In this study, 15% of the ORFs in the genome were screened and at least five factors involved in the regulation of photosystem stoichiometry were identified. The results suggest that more than 30 factors would be identified if all the ORFs of the genome were subjected to the analysis.

CHAPTER II

The quantitative analysis of the induction kinetics of chlorophyll fluorescence of cyanobacterial mutants cells

INTRODUCTION

As a tool to monitor the condition or location of the cellular process, fluorescent probes have been widely used in biological research. Improvement of fluorescent dyes and microscopy, together with the accumulation of genome information, enable us to elucidate the function of each gene systematically. For example, green fluorescent protein fusion proteins were systematically constructed in *Saccharomyces cerevisiae*, and genes were classified into 22 distinct subcellular categories (Huh et al. 2003). Although the difficulty still remains in obtaining quantitative results of the protein localization, this kind of technique is quite valuable for the large-scale analysis. Microarray analysis is another example of the fluorescence application in biology: cDNA that labeled by fluorescent dyes was used for the quantification of the gene expression levels. Among the mass production of post genomic data, no other methodological approach has transformed molecular biology more in recent years than the use of microarray (Hoheisel, 2006). Microarray have good reproducibility that can be achieved across laboratories and platforms (Larkin et al. 2005). It is relatively easy to extract quantitative data because microarray data themselves are expressed as intensity of fluorescence. However, these methods always require transformation of cells or labeling of DNAs to introduce fluorescent dye into systems.

On the other hand, photosynthetic organisms possess a natural fluoresce probe, chlorophyll, which is essential for photosynthesis. Chlorophyll fluorescence reflects redox state of photosynthetic transport. Thus, not only the location of the chlorophyll, but also the condition of photosynthesis can be evaluated by its fluorescence. Chlorophyll fluorescence is also suitable for quantitative analysis because it can be detected by simple optic devises such as photomultiplier, photodiode or CCD camera. In plant cells, photosynthesis is conducted in chloroplasts so that chlorophyll fluorescence principally reflects the condition of photosynthesis. However, the situation must be different in the case of cyanobacteria, which is photosynthetic prokaryote. Since cyanobacterial cells are not separated by organelles, cyanobacterial chlorophyll fluorescence reflects not only photosynthesis but also other metabolic systems, at least theoretically. Therefore, I assume that chlorophyll fluorescence emitted from cyanobacteria could be considered as informative data on many cellular processes. In Chapter I, traits of chlorophyll fluorescence kinetics were used to obtain the information on photosystem stoichiometry. However, the fluorescence data were compared with the judgment by eye, so that it is difficult to apply this method to other purposes. In this chapter, I employ quantitative phenotyping of

cyanobacterial mutants. By the quantitative re-analyses of the data set obtained in Chapter I, several pieces of new information were obtained. The results obtained here would open the way to apply the chlorophyll fluorescence to the elucidation of cellular metabolism other than photosynthesis.

MATERIALS AND METHODS

Calculation of dissimilarities

The relative fluorescence intensity at time t of mutant A, $F_A(t)$, is given by

$$F_A(t) = f_A(t)/f_A(0),$$

where $f_A(t)$ is the absolute fluorescence intensity at time t of mutant A, $f_A(0)$ is the initial absolute fluorescence intensity of mutant A. To compare mutants on different plates, the normalized relative fluorescence intensity, $nF_A(t)$, is defined as

$$nF_A(t) = F_A(t)/F_{WT}(t),$$

where $F_{WT}(t)$ is the relative fluorescence intensity of the wild type on the same plate that mutant A is spotted. The simple dissimilarity between mutant A and mutant B, sD(A, B), is calculated as

$$sD(A,B) = \sum_{t=0}^{134}((nF_A(t) - nF_B(t))^2).$$

Several weighting functions were devised to analyze specific characteristics of the dissimilarity. The weighting function that become sequentially lighter with time t, eW(t), is defined as

$$eW(t)=(135-t)^4.$$

This weighting function gives weight on the early phase of the fluorescence induction. Using this weighting function, the early-phase weighted dissimilarity between mutant A and mutant B, eD(A,B), is calculated as

$$eD(A,B) = \sum_{t=0}^{134}((eW(t)\times(nF_A(t) - nF_B(t)))^2).$$

Another weighting function was designed to extract the common characteristics of the fluorescence kinetics of the two mutants that show similar fluorescence kinetics. The heavier weight is assigned to the points where 1) mutant C and mutant D behaves similarly, 2) mutant C and WT behaves differently, and 3) mutant D and WT behaves differently. This mutant-specific weighting function, mW(t) is defined as

$$mW(t) = \sqrt{\frac{e^{(|nF_C(t)-nF_{WT}(t)|)} \times e^{(|nF_D(t)-nF_{WT}(t)|)}}{e^{(|nF_C(t)-nF_D(t)|)}}}$$

and the mutant-specific weighted dissimilarity is calculated as

$$mD(A,B) = \sum_{t=0}^{134}((mW(t)\times(nF_A(t) - nF_B(t)))^2).$$

In this study, this weighting function was mainly used to extract mutants that shows similar fluorescence kinetics with that of *sll1961* mutant and

pmgA mutant. Therefore, I used *sll1961* mutant and *pmgA* mutant as mutant C and D in the above equation, and dissimilarity was calculated between *sll1961* mutant (mutant A in the above equation) and all the other mutants (mutant B in the above equation).

Statistical analysis

Cluster analyses were performed in R (Ihaka, R., and Gentleman, R. 1996), a system for statistical computation and graphics. R (Version 2.0.1) ran under MacOS X (Version 10.2.8). It is available freely via CRAN, the Comprehensive R Archive Network, whose master site is at http://www.R-project.org. All the clustering algorithms can be found in R in the base package.

Database

All phenotype data were stored into a relational database using MySQL. Tabular structure for phenotypic description consists of the mutant ID, disrupted ORF ID, transposon insertion sites. Digitalized fluorescence intensity kinetics data are stored as text files linked to mutant IDs. Positions of transposon insertion were determined by BLASTN searches against *Synechocystis* genome sequences of the CyanoBase.

RESULTS

Mathematical feature of chlorophyll fluorescence kinetics of the wild type

Fig. 2-1A and Fig. 2-1B show same chlorophyll fluorescence kinetics normalized at the initial level of the fluorescence observed in the wild type grown under high light condition. Chlorophyll fluorescence kinetics of the wild type grown under high light condition was fitted to the function described below with a correlation coefficient of 0.9986 by nonlinear least-squares curve fitting.

$$y = 50.8 \times e^{\left(-e^{(-5.08\times(x-0.272))}\right)} + 48 \times 2^{\left(-\frac{x}{1.09}\right)} - \frac{8.09}{x \times 0.489} e^{\left(\frac{-\left(\ln\left(\frac{x}{1.3}\right)\right)^2}{2\times 0.489^2}\right)} + 55.5 - 18.6 \times 2^{\left(-\frac{x}{11.9}\right)}$$

(y :fluorescence intensity, x : time (s))

It should be noted that this equation is purely empirical, and there is no theoretical background in the precise kinetics of chlorophyll fluorescence. The causes of the time course change in the chlorophyll fluorescence is more or less elucidated qualitatively, but nobody can fully explain the kinetics quantitatively. The function given above consists of exponential functions, and the data points of the earlier phase have more information than the later phase. Moreover, fluctuation of the data in multiple experiments is larger in the later phase. Considering these factors and also to shorten the time for calculation in the following analysis, the data points are reduced from the 1126 to 135 points by averaging data points at later phase (Fig. 2-1C,D). In the time range of 0-1 s, 1-3

s, 3-7 s, 7-15 s, 15-31 s and 31-45 s, one data points were calculated by averaging every one, two, four, eight, sixteen and thirty-five data points, respectively. The equation shown above is a function of 10 parameters. The results suggest that the complexity of the fluorescence kinetics could be described by the combination of 10 parameters, although the equation itself is only valid for the description of the fluorescence kinetics of the wild type strain.

Dissimilarities between sll1961 mutant and the other mutants

To analyze the fluorescence kinetics, I first paid attention to peaks and troughs of the induction curves. However, not only the position and height of the peaks, but also the number of peaks was different among mutants. The overall shape of the fluorescence kinetics is totally disturbed in some mutants, and the complexity of the kinetics varied from one mutant to another. Fig. 2-2 shows examples of kinetics emitted from several mutants. It should be mentioned that *appC*, *pgt*, *pilC* and *glcE* are non-photosynthetic genes that encode ABC-type oligopeptide transport system permease protein, pteridine glycosyltransferase, pilin biogenesis protein and glycolate oxidase subunit, respectively. Considering the changes in the complexity of the chlorophyll fluorescence kinetics, I applied less empirical methods to analyze the data. My method was based on the idea that the deviations of relative chlorophyll fluorescence intensities at one time point could be used as a phenotype of the mutant. To quantify the "phenotype", sum of the squared deviations of fluorescence intensities at every time point between the *sll1961* mutant and other mutants was calculated and defined as the simple dissimilarity (for details, see Materials and Methods). When mutants were listed by the order of the simple dissimilarity, *sll1028*, *slr1136*, *slr0645* and *slr1138* mutants, which were identified in Chapter I, were ranked in the first, second, fourth and fifth position in the list for high-light grown cells, respectively (Table 2-1). Thus, I conclude that this simple dissimilarity reflects the "shape" of the chlorophyll fluorescence kinetics, and could be used for the quantitative analysis of the mutant phenotype. However, *pmgA* (*sll1968*) and *slr0249* mutants were not ranked high on the list of the simple dissimilarity: the two mutants were ranked at 125th and 375th in the list (Table 2-1), although the fluorescence kinetics of the two mutants looks quite similar to that of *sll1961* mutant. The simple dissimilarity could be a measure of the mutant phenotype, but not sufficient to search for all of the mutants I picked up by eye in the Chapter I. Thus another feature extraction algorithm would be necessary.

Although fluorescence kinetics of *sll1961* mutant was quite similar to *pmgA* mutant until around 1 second, the difference between the two sets of fluorescence kinetics increased with time. In the view of this time dependent difference, I set weights that become sequentially lighter with time before the summing squared deviations. The early-phase weighted dissimilarities of all the mutants against *sll1961* mutant were calculated (Table 2-2). Candidates identified in Chapter I and *pmgA* mutant were high on the rank of the early-

phase weighted dissimilarities in the case of high-light grown cells. The early-phase weighted dissimilarity of the photosystem stoichiometry related mutants grown under low-light condition were more widely distributed in the list than that of mutants grown under high-light condition, in agreement with the mild phenotype in the low-light grown cells of these mutants (Table 2-2, Fig. 2-3A(2), B(2)). Thus, the early-phase weighted dissimilarity is useful quantitative parameter, and could be used successfully to collect the mutants with fluorescence kinetics similar to that of *sll1961* mutant. However, there is also a problem in this early-phase weighted dissimilarity. There is no theoretical background in the selection of weight and the result would become different when different weight is applied. This method is based on the weight that set manually, and cannot be regarded as an objective one.

Therefore, I tried another algorithm. Common part of the fluorescence kinetics of *sll1961* and *pmgA* mutants would have information about increased PSI/PSII ratio and different part of the fluorescence kinetics would contain information peculiar to either *sll1961* mutant or to *pmgA* mutant. Therefore, I set the heavier weight for the point where the relative fluorescence intensity is similar between *sll1961* mutant and *pmgA* mutant. The mutant-specific weight dissimilarity yielded similar results to the early-phase weight dissimilarity (Table 2-3, Fig. 2-3B(2), B(3)). Thus, the mutant-specific dissimilarity is as effective as early-phase dissimilarity to pick up similar fluorescence kinetics to that of *sll1961* mutant. Some mutants in the list of the mutant-specific weight dissimilarity ranked as high as the known mutants defective in the regulation of the photosystem stoichiometry. They could be candidates for the mutants that have defect in the regulation of photosystem stoichiometry. It must be stressed that the dissimilarity with the mutant-specific weight is calculated automatically. If the two mutants of interest are given, the weight can be calculated without any personal consideration. The method could be used not only for the photosystem stoichiometry mutants, but also for any other mutants of interest.

Hierarchical cluster analysis of mutant-specific weighted dissimilarities

I performed a hierarchical clustering of mutants by mutant-specific weighted dissimilarities used above by Ward's method in order to pick up the mutants that show similar chlorophyll fluorescence kinetics with that of the known mutants with modified photosystem stoichiometry. *pmgA* mutant, *sll1961* mutant and the candidates identified in chapter I that grown under high-light condition were closely assembled on the dendrogram (Fig. 2-4A). The same mutants were more widely distributed when the dataset from the cells grown under low light condition was used (Fig. 2-4B) compared with those from cells grown under high-light condition. Mutants located near the known photosystem stoichiometry mutants in the dendrogram are the candidates for mutants with modified photosystem stoichiometry.

Determination of photosystem stoichiometry by measuring fluorescence spectra at liquid nitrogen temperature

Clustering of mutants based on the dissimilarities yielded candidates for the mutants with modified photosystem stoichiometry. I picked up nine mutants from those candidates, and determined fluorescence emission spectra of those mutants at liquid nitrogen temperature, in order to detect possible modification in photosystem stoichiometry (Fig. 2-5). Three of the nine mutants showed higher PSI/PSII ratio when grown under high light condition. Under low light condition, however, these three mutants did not exhibit any significant difference in PSI/PSII ratio compared with the wild-type cells. Another two mutants showed lower PSI/PSII ratio than the wild type under low-light condition while the difference is insignificant under high light condition. The remaining four mutants did not show any significant difference from the wild type both under high-light condition and low-light condition.

Frequency distribution of dissimilarities

When frequency distribution of simple and mutant-specific dissimilarities was calculated against the mutant of *sll1961* as an object (Fig. 2-6C, D, G and H), the peak is much higher and narrower compared with that calculated against the wild type as an object (Fig. 2-6A, B, E and F). The result suggests that the chlorophyll fluorescence kinetics of *sll1961* mutant differs markedly from that of the wild type, and most of the mutants have less distinct phenotypes. In fact, the simple dissimilarities of 30 mutants were higher than that of *sll1961* mutant (1698.26) in the case of the cells grown under high-light condition. This raises a question: Is it possible that the phenotype of the *sll1961* mutant is exceptionally strong, and only about 30 mutants could be analyzed by the fluorescence kinetics? To estimate the validity of the method, it must be necessary to determine the variance of the phenotype among cultures of wild type cells.

Frequency distribution of the simple dissimilarities of 16 independent cultures of the wild type was compared to that of the mutants using the average of the 16 wild type cultures as an object of dissimilarity calculation (Fig. 2-6). When cells were grown under low-light condition, the maximum of simple dissimilarity calculated for the 16 independent cultures of the wild type was 44.12. Under the same condition, 340 mutants in the mutant library showed the simple dissimilarity over 44.12. Thus, I assume that 68% of the mutant phenotype could be analyzed by the simple dissimilarity with cells grown under low light condition. In the case of high-light grown cells, the maximum of the simple dissimilarity was 143.82 in 16 independent cultures of the wild type. Since this value is considerably larger than the value obtained with low light grown cells, variance of the cell condition is much bigger in high-light grown cells than in low-light grown cells. 225 mutants in the mutant library showed dissimilarity over 143.82. Accordingly, I assume that 45% of the mutants could

be analyzed by the simple dissimilarity with cells grown under high-light condition.

Relationship between dissimilarity and gene expression profile

It is natural to assume that the mutants of genes that expressed under specific condition show phenotypes only under such condition. Now I can quantify the degree of phenotype as the change in chlorophyll fluorescence. The dissimilarity between each mutant and the wild type strain could be used as a measure of the severity of the phenotype so that the hypothesis could be directly tested by the comparison of gene expression profiling and dissimilarity profiling (Fig. 2-7). For this comparison, I used microarray analysis data reported by Hihara et al. 2001, since they determined the mRNA expression profile under high-light condition as well as low-light condition. Moreover, the genetic background used in their study is the same as that used in this study. When the ratio of dissimilarities between high-light condition and low-light condition was plotted against the ratio of mRNA expression level between the two light conditions in logarithmic scale, I found that all the genes that exhibited an increase of more than three times in mRNA expression also exhibited a significant increase in dissimilarity ratio of the mutants. However, it must be noted that most of the genes are expressed equally under low- or high-light condition irrespective of the large variation in the dissimilarity ratio.

Effect of photosynthetic inhibitors on chlorophyll fluorescence kinetics

Inhibitors decrease the rate of biochemical reactions. Thus, the effect of inhibitors would mimic the disruption of genes that are responsible for such biochemical reactions. DCMU inhibits photosynthesis by blocking electron transport from Q_A to Q_B in PSII. Upon the addition of DCMU, relative chlorophyll fluorescence intensity decreased by concentration-depending manner (Fig. 2-8A). MV is an artificial electron acceptor of PSI. Decrease of fluorescence intensity at the first peak was caused by the addition of MV and the effect of MV was also dependent on concentration (Fig. 2-8B). The result suggests that first peak of the fluorescence kinetics is caused by the rate limiting of electron transfer at downstream of PSI. The concentration dependent changes in the fluorescence kinetics indicate that change in the chlorophyll fluorescence is not caused in all-or-none, but quantitatively.

DISCUSSION

Quantitative approach to analyze fluorescence kinetics

The simple dissimilarity was first applied to compare the chlorophyll fluorescence kinetics. This approach seems to be effective to some extent because *ccmk2*, *ctaCI*, *slr0645*, *ctaEI* and *sll1916* mutants were picked up by this method. However, the simple dissimilarities of *sll1968* and *slr0249* mutants were larger than the smallest value of that of the sixteen independently cultured

strains of the wild type (Fig. 2-3B(1) and Table 2-1). The early-phase weighted dissimilarity is a better index than the simple dissimilarity: all the mutants analyzed in Chapter I was found to be ranked high on the list of dissimilarity calculated against the *sll1961* muntant (Fig. 2-3B(2) and Table 2-2). Weighting function would be a powerful method to search for mutants that show similar chlorophyll fluorescence kinetics to this specific mutant. However, the early-phase weighting is not necessarily a best method for other mutants than the *sll1961* mutant. Some mutants may be characterized by the feature in late-phase of the fluorescence kinetics. There is no inevitability in the determination of the weight in early-phase dissimilarity. To avoid subjective treatment of the data, I employed the mutant-specific weighting. The mutant-specific weighting is equally effective with the early phase weighting (Fig. 2-3B(2), (3) and Tables 2-2, 2-3). Furthermore, the weight is determined solely by the fluorescence kinetics of the two mutants, and there is no room for the subjective manipulation of the parameter. Thus, the mutant-specific weighted dissimilarity would be a good quantitative parameter for the practical analysis of different types of fluorescence kinetics.

My study represents the first *in silico* screening of candidates that shows modified photosystem stoichiometry using the quantitative characterization of the chlorophyll fluorescence kinetics. This approach was quite effective, and three of nine mutants with smaller dissimilarity than *slr0645* mutant showed defect in the regulation of photosystem stoichiometry under high-light condition. The quantitative analysis is much better than previous qualitative analysis: the four mutants isolated by this method were not discernible to my eyes and could not be selected by the simple comparison of the "shape" of the fluorescence kinetics.

Out of the remaining six mutants, two mutants showed the modified photosystem stoichiometry only under low-light condition. This characteristics is similar to that observed for *slr0249* mutant (Chapter I). Thus, it is apparent that the mutants with similar characteristics to *slr0249* mutant also show *sll1961*-type fluorescence kinetics, and ranked high in the dissimilarity list of *sll1961* mutant (Table 2-3). Although the mutants identified in this study showed several different phenotypes as to photosystem stoichiometry, i.e. high PSI under high light, low PSII under high light or low PSI under low light, all the mutants had common phenotype in the fluorescence kinetics. It could be postulated that the dissimilarity rank of chlorophyll fluorescence against the *sll1961* mutant would reflect imbalance of photosystem activity. Many photosystem stoichiometry mutants showed lower PSII or higher PSI under high-light condition compared with wild type strain. Some mutants including *slr0249* mutant are exceptions, but *slr0249* mutants exhibited lower PSII efficiency (i.e. lower Fv/Fm) than the wild type, although the difference may not be statistically significant (CHAPTER I, Table 1-3). It is tempting to assume that the fluorescence kinetics reflect either relative amount or relative activity of two

photosystems.

The factors involved in the regulation of photosystem stoichiometry

In response to elevated photon flux density, photosynthetic organisms change their photosynthetic apparatus to maintain a balance between energy supply (light harvesting and electron transport) and consumption (CO_2 fixation), and to avoid potential photodamage. This widely observed and physiologically important process, termed acclimation to high light, has been extensively investigated from the physiological point of view. Regulation of photosystem stoichiometry is also affected by a loss of gene function (Hihara et al.1998, Fujimori et al.2005, Nomura et al. 2006, Chapter I of this study). In this chapter, I found that three mutants, *crtO*, *ycf4* and *slr0172* mutants could only insufficiently decrease PSI (or increase PSII) under high-light condition. *crtO* mutant cannot synthesize echinenone from β-carotene and PSII activity of the mutant is decreased by high-light treatment (Schafer et al. 2005). High PSI/PSII ratio of *crtO* mutant would reflect the decreased amount of PSII under high-light condition. The high PSI/PSII ratio under high-light condition might be a side-effect from the increased photodamage of PSII rather than lack of ability to modulate photosystem stoichiometry.

ycf4 mutants was reported that the level of PSII was higher and that of PSI was lower in the mutants grown under 40 μmol photons m^{-2} s^{-1} compared with the wild type strain (Wilde et al. 1995). In this study, *ycf4* mutant showed the normal photosystem stoichiometry after acclimation to low-light condition (20 μmol photons m^{-2} s^{-1}). After acclimation to high-light condition (200 μmol photons m^{-2} s^{-1}) for 24 h, however, the mutant showed higher PSI/PSII ratio. *ycf4* mutant might change its photosystem stoichiometry according to its environmental photon flux density. In a green alga, *Chlamydomonas reinhardtii*, the homolog of the *ycf4* gene served for the assembly of the PSI reaction center complexes (Boudreau et al. 1997). At first glance, this reported phenotype contradicts higher relative PSI content observed in this study. However, there is a possibility that the PSI complexes in the *ycf4* mutant lacks some component(s) due to the defect in the assembly process, and the content of PSI increased to compensate the defect in PSI activity. More close examination of the components, activity and quantity of PSI would be necessary for the mechanism of the modulation of PSI content.

Finally, *slr0172* encodes hypothetical protein with CBS domain pair. In some cases, CBS domains may act as sensors of cellular energy status by being activated by AMP and inhibited by ATP. It is possible to assume that the regulation of photosystem stoichiometry is achieved through the sensing of energy status, which should be affected by the photon flux density of the environment. Although the physiology of the modulation of photosystem stoichiometry has been extensively studied in the past 30 years, the sensing mechanism of light condition is still obscure. The characterization of *slr0172*

would become a breakthrough for the elucidation of the sensing mechanism.

Strength of phenotype and its effect on dissimilarity

The ratio of PSI/PSII in *slr0645* mutant under low-light condition was significantly higher than that in the wild type (Fig. 1-4A). However, *slr0645* mutant was not ranked high in the lists of weighted dissimilarity compared with the other mutants having defect in the regulation of photosystem stoichiometry (Tables 2-2 and 2-3). The result of cluster analysis (Fig. 2-4B) showed similar tendency, and the *slr0645* mutant located rather far from the other mutants that have defect in the regulation of photosystem stoichiometry. It is clear from the experiment with photosynthetic inhibitors (Fig. 2-8) that chlorophyll fluorescence kinetics is quantitative phenotype. Taking this into consideration, the chlorophyll fluorescence kinetics of *slr0645* mutant under low light (Fig. 1-2B) could be regarded as a weak phenotype compared with the other photosystem stoichiometry mutants. The "shape" of the fluorescence kinetics of the *slr0645* mutant is quite similar to the other photosystem stoichiometry mutants, but the dissimilarity between the *slr0645* mutant and the wild type is smaller, resulting in the low rank in the dissimilarity list. Furthermore, the higher similarity between the *slr0645* mutant and the wild type prevent the clustering of the *slr0645* mutant and the other photosystem stoichiometry mutants, since the number of the mutants showing phenotype similar to the wild type is quite large. To analyze the mutants with weak phenotype, different statistical approach would be necessary.

FUTURE PERSPECTIVE

In this study, I collected a large amount of kinetic data by monitoring the time course changes of chlorophyll fluorescence intensity in 500 mutants and the wild type of *Synechocystis* sp. PCC 6803. Similarity of the fluorescence kinetics was applicable for the use in screening for mutants that have defect on the modulation of photosystem stoichiometry. Moreover, when one has the two chlorophyll fluorescence kinetic data for specific phenotype at hand, one could search for desired mutants by the mutant-specific weighted dissimilarity *in silico*. This quantitative and objective parameter allowed me to pick up three novel photosystem stoichiometry related mutants.

Chlorophyll fluorescence kinetics was affected by many gene disruptions even if the disrupted genes were not directly involved in photosynthesis. For example, respiratory components such as cytochrome *c* oxidase were shown to affect the fluorescence kinetics. I assume that the method developed here could be used not only for the screening of photosynthesis related genes but also for the screening of genes of the wide range of function. This is mainly based on the advantage of cyanobacteria as experimental organisms. Cyanobacteria are prokaryotes, and the cells are not divided into organelles. Thus, the different metabolisms of the cyanobacterial cells could interact with photosynthesis. This situation cannot be expected in higher plants. Moreover, the redundancy of the gene function would be more prominent in higher plants than in cyanobacteria. Thus, the application of the method developed in this study is restricted in cyanobacteria at present. In future, I would like to develop the different fluorescent probes that monitor the metabolic condition of different organelles. The recent development of fluorescent probes enables us to monitor the conformation of many proteins. It may be possible to construct fluorescence probes that monitor the electron transfer of the respiratory chain. That would be a first step for my future project.

Cyanobacteria have about 3200 genes on their genomes, and about half of them are of unknown function. My quantitative phenotype analysis reveals that disruption of about half of the genes in cyanobacteria affect chlorophyll fluorescence kinetics. Therefore, among the 1600 cyanobacterial genes of unknown function, 800 genes could be analyzed by the chlorophyll fluorescence, theoretically. However, there are apparent difficulties in actual analysis. As revealed in Chapter II, many mutants showed similar phenotype with the wild type strain. Even if the phenotypic difference between mutants and the wild type is statistically significant, genes with weak phenotype could not be clustered with the ones with strong phenotype as discussed in Chapter II. To solve this difficulty, it may be possible to use the direction of the change in the phenotype instead of using the direct value of the phenotype. This type of mathematical treatment reduced the quality of information in the dataset, but may be effective to cluster the genes with same function irrespective of the strength of the phenotype. Such approach would be also tested in future.

REFFERENCES

Altschul, S.F., Madden, T.L., Schaffer, A.A., Zhang, J., Zhang, Z., Miller, W. and Lipman, D.J. (1997) Gapped BLAST and PSI-BLAST: a new generation of protein database search programs. *Nucleic Acids Res.* 25: 3389-3402.

Arnon, I.D., McSwain, B.D., Tsujimoto, H.Y. and Wada, K. (1974) Photochemical activity and components of membrane preparations from blue-green algae. I. Coexistence of two photosystems in relation to chlorophyll a and removal of phycocyanin. *Biochim. Biophys. Acta* 357: 231-245.

Barabasi, A.L. and Oltvai, Z.N. (2004) Network biology: understanding the cell's functional organization. *Nat. Rev. Genet.* 5: 101-113.

Boudreau, E., Takahashi, Y., Lemieux, C., Turmel, M. and Rochaix, J. D. (1997) The chloroplast ycf3 and ycf4 open reading frames of Chlamydomonas reinhardtii are required for the accumulation of the photosystem I complex. *EMBO J.* (16): 6095-6104.

Buchanan, B.B. and Luan, S. (2005) Redox regulation in the chloroplast thylakoid lumen: a new frontier in photosynthesis research. *J Exp Bot.* 56: 1439-1447.

Cannon, G.C., Bradburne, Heinhorst, S., Bradburne, C.E. and Shively, J.M (2002) Carboxysome genomics: a status report. *Funct. Plant Biol.* 29: 175-182.

Chow, W.S., Melis, A. and Anderson, J.M. (1990) Adjustments of photosystem stoichiometry in chloroplasts improve the quantum efficiency of photosynthesis. *Proc. Natl Acad. Sci. USA* 87: 7502-7506.

de Jesus Ferreira, M.C., Bao, X., Laize, V. and Hohmann, S. (2001) Transposon mutagenesis reveals novel loci affecting tolerance to salt stress and growth at low temperature. *Curr. Genet.* 40: 27-39.

Flores, E., Frias, J.E., Rubio, L.M. and Herrero, A. (2005) Photosynthetic nitrate assimilation in cyanobacteria. *Photosynth. Res.* 83: 117-133.

Fujimori, T., Higuchi, M., Sato, H., Aiba, H., Muramatsu, M., Hihara, Y. and Sonoike, K. (2005) The mutant of *sll1961*, which encodes a putative transcriptional regulator, has a defect in regulation of photosystem stoichiometry in the cyanobacterium *Synechocystis* sp. PCC 6803. *Plant Physiol.* 139: 408-416.

Fujita, Y., Ohki, K. and Murakami, A. (1985) Chromatic regulation of photosystem composition in the photosynthetic system of red and blue-green algae. *Plant Cell Physiol.* 26: 1541-1548.

Fujita, Y (1997) A study on the dynamic features of photosystem stoichiometry: accomplishments and problems for future studies. *Photosynth. Res.* 53: 83–93.

Gantt, E. (1994) in The Molecular Biology of Cyanobacteria, ed. Bryant, D. A. (Kluwer, Dordrecht, The Netherlands), pp. 119-138.

Geoffroy, M.C., Floquet, S., Metais, A., Nassif, X. and Pelicic, V. (2003) Large-scale analysis of the *meningococcus* genome by gene disruption: Resistance to complement-mediated lysis. *Genome Res.* 13: 391-398.

Govindjee (1995) Sixty-three years since kautsky: chlorophyll a fluorescence. *Aust. J. Plant Physiol.* 22: 131-160.

Hart, S.E., Schlarb-Ridley, B.G., Bendall, D.S. and Howe, C.J. (2005) Terminal oxidases of cyanobacteria. *Biochem. Soc. Trans.* 33(Pt 4): 832-835.

Hashimoto, M., Endo, T., Peltier, G., Tasaka, M. and Shikanai, T. (2003) A nucleus-encoded factor, CRR2, is essential for the expression of chloroplast *ndhB* in *Arabidopsis*. *Plant J.* 36: 541-549.

Hervas, M., Navarro, J.A. and De La Rosa, M.A. (2003) Electron transfer between membrane complexes and soluble proteins in photosynthesis. *Acc. Chem. Res.* 36: 798-805.

Hihara, Y. and Ikeuchi, M. (1997) Mutation in a novel gene required for photomixotrophic growth leads to enhanced photoautotrophic growth of *Synechocystis* sp. PCC 6803. *Photosynth. Res.* 53: 243-252.

Hihara, Y., Sonoike, K. and Ikeuchi, M. (1998) A novel gene, *pmgA*, specifically regulates photosystem stoichiometry in the cyanobacterium *Synechocystis* species PCC 6803 in response to high light. *Plant Physiol.* 117: 1205-1216.

Hihara, Y., Kamei, A., Kanehisa, M., Kaplan, A. and Ikeuchi, M. (2001) DNA microarray analysis of cyanobacterial gene expression during acclimation to high light. *Plant Cell.* 13:793-806.

Hoheisel, J.D. (2006) Microarray technology: beyond transcript profiling and genotype analysis. *Nat Rev Genet.* 7:200-210.

Hope, A.B. (1993) The chloroplast cytochrome bf complex: a critical focus on function. *Biochim. Biophys. Acta.* 1143: 1-22.

Huh, W.K., Falvo, J.V., Gerke, L.C., Carroll, A.S., Howson, R.W., Weissman, J.S. and O'Shea, E.K. (2003) Global analysis of protein localization in budding yeast. 16;425: 686-91.

Hutchison, C.A., Peterson, S.N., Gill, S.R., Cline, R.T., White, O., Fraser, C.M., Smith, H.O., and Venter, J.C. (1999) Global transposon mutagenesis and a minimal *Mycoplasma* genome. *Science* 286: 2165-2169.

Ihaka, R., and Gentleman, R. (1996). R: A language for data analysis and graphics. *J. Comput. Graph. Stat.* 5: 299–314.

Jacobs, M.A., Alwood, A., Thaipisuttikul, I., Spencer, D., Haugen, E., et al. (2003) Comprehensive transposon mutant library of *Pseudomonas aeruginosa. Proc. Natl Acad. Sci. USA* 100: 14339-14344.

Kaneko, T., Sato, S., Kotani, H., Tanaka, A., Asamizu, E., et al. (1996) Sequence analysis of the genome of the unicellular cyanobacterium *Synechocystis* sp. strain PCC6803. II. Sequence determination of the entire genome and assignment of potential protein-coding regions. *DNA Res.* 3: 109-136.

Kawamura, M., Mimuro, M. and Fujita, Y. (1979) Quantitative relationship

between two reaction centers in the photosynthetic system of blue-green algae. *Plant Cell Physiol.* 20: 697-705.

Krause, G.H. and Weis, E. (1991) Chlorop hyll fluorescence and photosynthesis: the basics. *Annu Rev Plant Physiol Plant Mol Biol*, 42: 313–349.

Kufryk, G.I. and Vermaas W.F. (2006) Sll1717 affects the redox state of the plastoquinone pool by modulating quinol oxidase activity in thylakoids. *J. Bacteriol.* 188: 1286-1294.

Latimer, P., Bannister, T.T. and Rabinowitch, E. (1956) Quantum yields of fluorescence of plant pigments. *Science* 124: 585-586.

Lazar, D. (1999) Chlorophyll *a* fluorescence induction. *Biochim. Biophys. Acta* 1412: 1-28.

Larkin, J. E., Frank, B. C., Gavras, H., Sultana, R. and Quackenbush, J. (2005) Independence and reproducibility across microarray platforms. *Nature Methods* **2**, 337–344

Li, X.P., Bjorkman, O., Shih, C., Grossman, A.,R., Rosenquist, M., Jansson, S. and Niyogi, K.,K. (2000) A pigment-binding protein essential for regulation of photosynthetic light harvesting. *Nature* 403: 391-395.

Manodori, A. and Melis, A. (1984) Photochemical Apparatus Organization in *Anacystis nidulans* (Cyanophyceae) effect of CO_2 concentration during cell growth. *Plant Physiol.* 74: 67-71.

Manodori, A. and Melis, A. (1986) Cyanobacterial acclimation to photosystem I or photosystem II light. *Plant Physiol.* 82: 185-189.

Melis, A., Murakami, A., Nemson, J.A., Aizawa, K., Ohki, K. and Fujita, Y. (1996) Chromatic regulation in *Chlamydomonas reinhardtii* alters photosystem stoichiometry and improves the quantum efficiency of photosynthesis. *Photosynth. Res.* 47: 253-265.

Melis, A., Manodori, A., Glick R.E. Ghirardi, M.L., McCauley, S.W. and Neale, P.J. (1985) The mechanism of photosynthetic membrane adaptation to environmental stress conditions: a hypothesis on the role of electron-transport capacity and of ATP/NADPH pool in the regulation of thylakoid membrane organization and function. *Physiol. veg.* 23: 757-765.

Munshi, M.K., Kobayashi, Y. and Shikanai T. (2005) Identification of a novel protein, CRR7, required for the stabilization of the chloroplast NAD(P)H dehydrogenase complex in *Arabidopsis. Plant J.* 44: 1036-1044.

Munshi, M.K., Kobayashi, Y. and Shikanai, T. (2006) Chlororespiratory reduction 6 is a novel factor required for accumulation of the chloroplast NAD(P)H dehydrogenase complex in *Arabidopsis. Plant Physiol.* 141: 737-744.

Niyogi, K.K., Bjorkman, O. and Grossman A.R. (1997) *Chlamydomonas* xanthophyll cycle mutants identified by video imaging of chlorophyll fluorescence quenching. *Plant Cell* 9: 1369-1380.

Niyogi, K.K., Grossman, A.R. and Bjorkman, O. (1998) *Arabidopsis* mutants define a central role for the xanthophyll cycle in the regulation of

photosynthetic energy conversion. *Plant Cell* 10: 1121-1134.

Nomura, C.T., Persson, S., Shen, G., Inoue-Sakamoto, K., and Bryant, D.A. (2006) Characterization of two cytochrome oxidase operons in the marine cyanobacterium *Synechococcus* sp. PCC 7002: Inactivation of *ctaDI* affects the PS I:PS II ratio. *Photosynth. Res.* 87: 215-28.

Paillotin G. (1976) Capture frequency of excitations and energy transfer between photosynthetic units in the photosystem II. *J. Theor. Biol.* 58: 219–235.

Pearson, W.R. (1998) Empirical statistical estimates for sequence similarity searches. *J. Mol. Biol.* 276: 71-84.

Renger, G. (2001) Photosynthetic water oxidation to molecular oxygen: apparatus and mechanism. *Biochim. Biophys. Acta.* 1503: 210-228

Rippka, R., Deruelles, J., Waterbury, J.B., Herdman, M. and Stanier, R.Y. (1979) Generic assignments, strain histories and properties of pure cultures of cyanobacteria. *J. Gen. Microbiol.* 111: 1-61.

Ross-Macdonald, P., Coelho, P.S., Roemer, T., Agarwal, S., Kumar, et al. (1999) Large-scale analysis of the yeast genome by transposon tagging and gene disruption. *Nature* 402: 413-418.

Salama, N.R., Sheperd, B. and Falkow, S. (2004) Global transposon mutagenesis and essential gene analysis of *Helicobacter pylori*. *J. Bacteriol.* 186: 7926-7935

Schafer, L., Vioque, A. and Sandmann, G. (2005) Functional in situ evaluation of photosynthesis-protecting carotenoids in mutants of the cyanobacterium *Synechocystis* PCC6803. *J Photochem. Photobiol. B.* (1):195-201.

Scherens, B. and Goffeau, A. (2004) The uses of genome-wide yeast mutant collections. *Genome Biol.* 5: 229.

Scherer, S., Almon, H. and Boger, P. (1988) Interaction of photosynthesis, respiration and nitrogen fixation in cyanobacteria. *Photosynth. Res.* 15: 95-114.

Sonoike, K. and Terashima, I. (1994) Mechanism of photosystem-I photoinhibition in leaves of *Cucumis sativus* L. *Planta* 194: 287-293.

Sonoike, K., Hihara, Y. and Ikeuchi, M. (2001) Physiological significance of the regulation of photosystem stoichiometry upon high light acclimation of *Synechocystis* sp. PCC 6803. *Plant Cell Physiol.* 42: 379-384.

Takahashi, T., Shimoi, H. and Ito, K. (2001) Identification of genes required for growth under ethanol stress using transposon mutagenesis in *Saccharomyces cerevisiae*. *Mol. Genet. Genomics* 265: 1112-1119.

Trissl, H.-W., Gao, Y. and Wulf, K. (1993) Theoretical fluorescence induction curves derived from coupled differential equations describing the primary photochemistry of photosystem II by an exciton-radical pair equilibrium. *Biophys. J.* 64: 974-988.

Wilde, A., Hartel, H., Hubschmann, T., Hoffmann, P., Shestakov, S. V. and Borner, T. (1995) Inactivation of a *Synechocystis* sp strain PCC 6803 gene

with homology to conserved chloroplast open reading frame 184 increases the photosystem II-to-photosystem I ratio. *Plant Cell.* (7): 649-658.

TABLES

Table 1-1. Category of the genes that is disrupted in the mutants of the library. Disrupted ORFs were classified into seventeen categories according to CyanoBase, and listed in the sections with titles representing categories. ND in "Low light" or "High light" columns indicates that chlorophyll fluorescence was not detected under indicated conditions.

ORF ID	Gene name	Low light	High light
Amino acid biosynthesis			
sll0080	*argC*		
sll1027	*gltD*		
sll1172	*thrC*		
sll1564			
sll1981	*ilvB*		ND
slr0036	*aspC*		
slr0084	*hisH*		
slr0212	*metH*		
slr0500	*hisB*		
slr0644			
slr0710	*gdhA*		
slr1022	*argD*		
slr1756	*glnA*		
slr1848	*hisD*		
slr2035	*proB*	ND	ND
slr2081	*tyrA*		ND
Biosynthesis of cofactors, prosthetic groups, and carriers			
sll0254			
sll0603	*menD*		
sll0794	*corR, coaR*		
sll0916	*cobH*		
sll1185	*hemF*		
slr0088	*crtO*		
slr0236			
slr0252		ND	ND
slr0492	*menE*		
slr0502	*cobW*		ND
slr0506	*por*		
slr0523			
slr0618	*cobQ*		

Table 1-1. Continued

ORF ID	Gene name	Low light	High light
slr0636			
slr1099	*ubiX*		
slr1269	*ggt*		
slr1293			
slr1777	*chlD*		
slr1784	*bvdR*	ND	ND
slr1882	*ribF*		
ssr0330	*ftrV*		ND
Cell envelope			
slr0191			
slr0495			
slr0938			
slr1271			
slr1874			
Cellular processes			
sll0616	*secA*		
sll0716			ND
sll1181			
sll1294			
sll1932	*dnaK*	ND	ND
sll1980	*trxA*		
sll1987	*cpx, katG*		
sll1988	*hsp33*		
slr0079			
slr0086			
slr0093	*dnaJ*		
slr0162	*pilC*		
slr0488			
slr0774	*secD*	ND	ND
slr0950			
slr1274	*pilM*		
slr1277			
slr1390	*ftsH*		
slr2102	*ftsY*		
ssl2922	*vapB*		

Table 1-1. Continued

ORF ID	Gene name	Low light	High light
Central intermediary metabolism			
sll0842			
sll1639	*ureD*		
slr0237			
DNA replication, restriction, modification, recombination, and repair			
sll0613	*ruvB*		
sll0766	*radC*		
sll0876	*ruvA*		
sll1143	*pcrA*		ND
sll1941	*gyrA*	ND	ND
slr0603	*dnaE*		
slr0707	*polA*		
slr0854	*phrA*		
slr0965	*dnaN*	ND	ND
Energy metabolism			
sll0045	*spsA*		
sll0053	*accC*		
sll0404	*glcD*		
sll0823			
sll0920	*ppc*		
sll1069			
sll1070			
sll1077	*speB2*		
sll1085	*glpD*	ND	ND
sll1178			
sll1189	*glcE*		
sll1196			
sll1212			
sll1299			
sll1682		ND	ND
sll1683			
slr0091			
slr0194	*rpiA*		
slr0329			

Table 1-1. Continued

ORF ID	Gene name	Low light	High light
slr0942			
slr0952	*fbpII*		
slr1020	*sqdB*		
slr1096			
slr1166	*pgt*		
slr1167	*gldA*		ND
slr1233			
slr1299			
slr1510	*plsX*		
slr1793			
slr2023	*fabD*		
slr2089	*shc*		
slr2132			
Hypothetical			
sll0082			
sll0148			
sll0154			
sll0160			
sll0180			
sll0185			
sll0230			
sll0350			
sll0456			
sll0470			
sll0471			
sll0488			
sll0597			
sll0602			
sll0608	*ycf49*		
sll0615			
sll0617	*vipp1*		
sll0661	*ycf35*		
sll0662			
sll0737			
sll0742			
sll0744			
sll0821	*cph2*		
sll0832			ND

Table 1-1. Continued

ORF ID	Gene name	Low light	High light
sll0839			
sll0858			
sll0913			
sll0996			
sll1002	*ycf22*		
sll1011			
sll1021			ND
sll1052			
sll1063			ND
sll1118			
sll1138			
sll1144			
sll1173			
sll1193			
sll1281	*psbZ, ycf9*		ND
sll1289			
sll1318			
sll1414			
sll1581			
sll1640			
sll1766			
sll1770			
sll1832			
sll1835			
sll1961			
slr0031		ND	ND
slr0082			
slr0172			
slr0179			
slr0181			
slr0197	*comA*		
slr0207			
slr0208			
slr0211			
slr0241			
slr0243			
slr0244			
slr0249			
slr0254			

Table 1-1. Continued

ORF ID	Gene name	Low light	High light
slr0263			
slr0269			
slr0317			ND
slr0337			
slr0351		ND	ND
slr0359			
slr0360			
slr0362			
slr0420			
slr0479			
slr0480	*ycf46*		
slr0491			
slr0605			
slr0630			
slr0637			
slr0645			
slr0650			
slr0765		ND	ND
slr0784			ND
slr0795	*nrsC*		
slr0852			
slr0863			
slr0865			
slr0869			
slr0889			
slr0959			
slr1035			
slr1048			
slr1050			
slr1081			ND
slr1094			
slr1097			
slr1100			
slr1102			
slr1104			
slr1114			
slr1117			
slr1128			
slr1143			

Table 1-1. Continued

ORF ID	Gene name	Low light	High light
slr1152		ND	ND
slr1170		ND	ND
slr1173		ND	ND
slr1194			ND
slr1206			
slr1218	*ycf39*		
slr1223			
slr1230			
slr1235			
slr1236			
slr1263			
slr1266			
slr1270			
slr1273			
slr1275			
slr1376			ND
slr1512	*sbtA*		
slr1519			
slr1557			
slr1677			
slr1692			
slr1721			
slr1753			
slr1911			
slr1913			
slr1914			
slr1917			
slr1923			
slr2013			
slr2032	*ycf23*		ND
slr2084			
slr2105		ND	ND
sml0011			
ssl0242			
ssl0259			
ssl0352			
ssl0353			
ssl0461			
ssl1923			

Table 1-1. Continued

ORF ID	Gene name	Low light	High light
ssr1473			ND
ssr1698			ND
ssr1765			ND
ssr2047			ND
ssr3341			ND
ssr3550		ND	ND
Other categories			
sll0086			
sll0163			
sll0217			
sll0219			
sll0222			
sll0245			
sll0395			
sll0829			ND
sll0915			
sll0990			
sll1032	*ccmN*		
sll1033			
sll1284			
sll1647		ND	ND
sll1664		ND	ND
sll1758			
sll1786	*tatD*		ND
sll1833			
sll1910	*zam*		
sll1945		ND	ND
sll1982			
sll1983			
slr0078			
slr0095			
slr0143	*hat*		
slr0201			
slr0265			
slr0604			
slr0697		ND	ND
slr0799		ND	ND
slr0857			

Table 1-1. Continued

ORF ID	Gene name	Low light	High light
slr0945			
slr0951			
slr1076			
slr1106			
slr1109			
slr1198			
slr1282			
slr1302	*cupB*		
slr1501			
slr1520		ND	ND
slr1682			
slr1761			
slr1916			
slr2047		ND	ND
slr2087	*ccs1, ycf44*		
slr2095			
slr2096			ND
Photosynthesis and respiration			
sll0223	*ndhB*		
sll0226	*ycf4*		
sll0741			
sll0849	*psbD*		
sll1028	*ccmK2*		
sll1030	*ccmL*		
sll1031	*ccmM*		
sll1182	*petC3*		
sll1322	*atpI*		
sll1323	*atpG*		
sll1324	*atpF*		
sll1326	*atpA*		
sll1578	*cpcA*		
slr0171	*ycf37*		
slr0261	*ndhH*		
slr0436	*ccmO*		ND
slr0844	*ndhF1*		
slr0851	*ndbA*		
slr1136	*ctaCI*		

Table 1-1. Continued

ORF ID	Gene name	Low light	High light
slr1138	*ctaEI*		
slr1291	*ndhD2*		
slr1311	*psbA2*		
slr2083	*ctaEII*		
sml0002	*psbX*		
smr0006	*psbF*	ND	ND
ssl0452	*nblA1*		
ssl2615	*atpH*		
ssr0390	*psaK1*		ND
Purines, pyrimidines, nucleosides, and nucleotides			
sll0757	*purF*		
slr0185			
slr0477	*purN*		
slr0838	*purM*		
slr1164			
Regulatory functions			
sll0039	*pixH, pisH*	ND	ND
sll0043	*pixL, taxAY1, hik18*		
sll0474	*hik28*		
sll0921			
sll1205			
sll1286			
sll1291			
sll1292			
sll1670		ND	ND
slr0073	*hik36*		
slr0081			
slr0152			
slr0210	*hik9*		
slr0222	*hik25*		
slr0240			
slr0321		ND	ND
slr0640	*hik27*		
slr0835			
slr0947	*rpaB, ycf27*		
slr1037			
slr1041			

Table 1-1. Continued

ORF ID	Gene name	Low light	High light
slr1042			
slr1147	*hik2*		
slr1212			
slr1214			
slr1285	*hik34*		
slr1305			
slr1324	*hik23*		
slr1325			
slr1393	*hik1*		
slr1416			
slr1489			
slr1759	*hik14*		
slr2100			
slr2104	*hik22*		
Transcription			
sll0856	*sigH*		
slr0080	*rnhA*		
slr0083	*crhR*		
slr1129	*rne*		
slr1130	*rhnB*		
slr1265	*rpoC1*		
Translation			
sll0078	*thrS*		
sll0179	*gltX*		
sll0454	*pheS*		
sll0467			
sll0830	*fus*		
sll1074	*leuS*		
sll1096	*rps12*	ND	ND
sll1097	*rps7*	ND	ND
sll1427			
sll1553	*pheT*	ND	ND
slr0033			
slr0164	*clpP4*		
slr0165	*clpP3*		
slr0193	*rbp3*		
slr0257	*ctpB*		

Table 1-1. Continued

ORF ID	Gene name	Low light	High light
slr0357	*hisS*		
slr0361			
slr0612			
slr0638	*glyQ*		
slr0744	*infB*		
slr0786			ND
slr0958	*cysS*		
slr1031	*tyrS*		
slr1331			ND
slr1703	*serS*		
ssl1426	*rpl35*	ND	ND
ssr1736	*rpl32*		ND
Transport and binding proteins			
sll0182			
sll0221			
sll0415			
sll0484			
sll0489			
sll0556			
sll0833		ND	ND
sll0912			
sll1041	*cysA*		
sll1102	*gtrA*	ND	ND
sll1180			
sll1202			
sll1204			
sll1206			
sll1406			
sll1409			
sll1762			
slr0074	*ycf24*		
slr0096			
slr0324	*appC*		
slr0369			
slr0944			
slr0949	*natD*		
slr1145	*gltS*		

Table 1-1. Continued

ORF ID	Gene name	Low light	High light
slr1149			
slr1200		ND	ND
slr1224			ND
slr1295	*futA1*		
slr1488			
slr1490			
slr1491			
slr1776		ND	ND
slr2043			
Unknown			
sll0156			
sll0188			
sll0225			
sll0238			
sll0243			
sll0252			
sll0394			
sll0403		ND	ND
sll0473			
sll0482			
sll0614			
sll0785		ND	ND
sll0857			
sll0910			
sll0914			
sll0980			
sll1006			
sll1068			
sll1086		ND	ND
sll1170			
sll1174			
sll1429			
sll1563			
sll1583			
sll1755			
sll1761			
sll1765			
sll1830			

Table 1-1. Continued

ORF ID	Gene name	Low light	High light
slr0069			
slr0145			
slr0151			
slr0168		ND	ND
slr0184			
slr0366			
slr0468			
slr0476			
slr0522			
slr0634			
slr0702			
slr0708			
slr0868			
slr0871			
slr0890			
slr1028			
slr1032			
slr1033			
slr1053			
slr1107			
slr1148			
slr1168			ND
slr1383			
slr1397			
slr1398			
slr1485			
slr1681			
slr1768			
slr1771			
slr1778			
slr1869			
slr2018			
slr2046			
ssl0323			
ssl1552			
ssr0335			ND
ssr2194			ND

Table 1-2. Anotations of the genes disrupted in the mutants that have altered photosystem stoichiometry.

ORF ID	gene name	annotation in Cyanobase	category	PSI/PSII	glucose sensitivity
sll1961		hypothetical protein	Hypothetical	high PSI (HL)	yes
sll1968	pmgA	photomixotrophic growth related protein	Other categories	high PSI (HL)	yes
sll1028	ccmK2	CO2 concentrating mechanism protein CcmK	Photosynthesis and respiration	high PSI (HL)	yes
slr1916		probable esterase	Other categories	high PSI (HL)	yes
slr1138	ctaEI	cytochrome c oxidase subunit III	Photosynthesis and respiration	low PSII (HL)	no
slr1136	ctaCI	cytochrome c oxidase subunit II	Photosynthesis and respiration	low PSII (HL)	no
slr0645		hypothetical protein	Hypothetical	low PSII (HL)	no
slr0249		hypothetical protein	Hypothetical	high PSII (LL)	no

Table 1-3. Fluorescence characteristics by PAM fluorometer. qP and qN were measured at 200 μmol m^{-2} s^{-1} both for low- and high-light grown cells. Values represent the average ±S.D. with three independent cultures.

	Fv/Fm	NPQ	qP	φII
Low light grown cells				
WT	0.50 ± 0.03	0.18 ± 0.03	0.57 ± 0.05	0.24 ± 0.05
sll1961	0.50 ± 0.06	0.14 ± 0.03	0.62 ± 0.08	0.26 ± 0.03
pmgA	0.51 ± 0.01	0.15 ± 0.01	0.51 ± 0.08	0.22 ± 0.03
ccmK2	0.51 ± 0.02	0.17 ± 0.03	0.50 ± 0.08	0.21 ± 0.03
slr1916	0.53 ± 0.00	0.16 ± 0.02	0.56 ± 0.13	0.25 ± 0.05
ctaEI	0.51 ± 0.04	0.18 ± 0.01	0.59 ± 0.07	0.25 ± 0.06
ctaCI	0.49 ± 0.02	0.18 ± 0.02	0.53 ± 0.08	0.21 ± 0.03
slr0645	0.50 ± 0.01	0.16 ± 0.01	0.55 ± 0.01	0.23 ± 0.02
slr0249	**0.42 ± 0.03**	0.15 ± 0.05	**0.29 ± 0.15**	**0.09 ± 0.05**
High light grown cells				
WT	0.53 ± 0.01	0.35 ± 0.04	0.53 ± 0.14	0.19 ± 0.03
sll1961	**0.45 ± 0.04**	**0.20 ± 0.04**	0.45 ± 0.13	0.15 ± 0.03
pmgA	**0.48 ± 0.00**	**0.25 ± 0.03**	0.51 ± 0.07	0.18 ± 0.02
ccmK2	**0.47 ± 0.01**	**0.25 ± 0.02**	0.55 ± 0.10	0.18 ± 0.04
slr1916	**0.45 ± 0.00**	**0.26 ± 0.03**	0.49 ± 0.20	0.15 ± 0.05
ctaEI	**0.50 ± 0.01**	0.34 ± 0.06	0.47 ± 0.09	0.16 ± 0.04
ctaCI	0.52 ± 0.02	0.32 ± 0.03	0.47 ± 0.06	0.17 ± 0.03
slr0645	0.51 ± 0.04	0.33 ± 0.02	0.50 ± 0.02	0.18 ± 0.03
slr0249	0.47 ± 0.07	0.33 ± 0.05	0.40 ± 0.14	0.12 ± 0.07

Table 2-1. Ranking of simple dissimilarities of mutants calculated against the *sll1961* mutant. ORF IDs of *pmgA* (*sll1968*) mutant and candidates for the photosystem stoichiometry mutnats obtained in chapter I are indicated in red.

	Low light			High light	
Rank order	Dissimilarity	ORF ID	Rank order	Dissimilarity	ORF ID
1	41.48	*slr1390*	1	196.38	*sll1028*
2	55.50	*slr0185*	2	293.47	*slr1136*
3	57.38	*slr1916*	3	359.91	*slr0612*
4	87.76	*slr0636*	4	404.35	*slr0645*
5	93.05	*slr0083*	5	658.13	*slr1138*
6	96.01	*sll1173*	6	748.52	*sll0219*
7	99.86	*slr0476*	7	749.25	*slr0604*
8	106.86	*ssl1552*	8	764.62	*sll0217*
9	122.63	*sll1028*	9	886.79	*slr1271*
10	127.83	*ssr1736*	10	887.46	*slr0240*
11	137.55	*slr0212*	11	905.68	*slr1114*
12	142.29	*sll0404*	12	909.31	*slr1916*
13	144.58	*slr0477*	13	920.01	*slr0710*
14	152.23	*sll0148*	14	944.92	*slr0708*
15	164.85	*slr1302*	15	952.43	*sll1406*
16	199.43	*slr1031*	16	958.35	*slr0145*
17	212.69	*sll1143*	17	965.52	*slr1793*
18	226.84	*slr0211*	18	980.25	*slr1311*
19	229.66	*slr1271*	19	980.99	*slr0630*
20	229.87	*slr0357*	20	999.34	*sll0608*
21	249.82	*slr0603*	21	1004.28	*slr0500*
22	271.37	*slr0181*	22	1009.96	*slr2018*
23	273.51	*slr1911*	23	1019.95	*ssl0259*
24	274.50	*slr2023*	24	1053.06	*slr0637*
25	291.90	*sll0716*	25	1085.24	*sll1429*
26	292.38	*slr0838*	26	1093.31	*slr0263*
27	298.32	*sll1181*	27	1100.38	*slr1223*
28	300.69	*ssr0330*	28	1125.91	*ssl0242*
29	313.43	*sll1011*	29	1134.49	*sll0252*
30	322.23	*sll1052*	30	1144.20	*slr1274*
⋮	⋮	⋮	⋮	⋮	⋮
70	515.90	*slr1138*	125	1560.58	*sll1968*
⋮	⋮	⋮	⋮	⋮	⋮
85	580.03	*sll1968*	375	2802.33	*slr0249*
⋮	⋮	⋮	⋮	⋮	⋮
137	764.42	*slr0645*			
⋮	⋮	⋮			
156	799.99	*slr1136*			
⋮	⋮	⋮			
475	7659.02	*slr0249*			
⋮	⋮	⋮			

Table 2-2. Ranking of early-phase weighted dissimilarities of mutants calculated against the *sll1961* mutant. ORF IDs of *pmgA* (*sll1968*) mutant and candidates for the photosystem stoichiometry mutnats obtained in chapter I are indicated in red.

	Low light			High light	
Rank order	Dissimilarity	ORF ID	Rank order	Dissimilarity	ORF ID
1	9.76	*slr1916*	1	15.62	*sll1968*
2	10.91	*slr0636*	2	19.20	*slr0172*
3	11.41	*sll1052*	3	24.31	*sll1028*
4	13.79	*slr0185*	4	32.13	*slr1138*
5	15.55	*slr0645*	5	36.57	*slr1136*
6	16.62	*slr1224*	6	52.84	*sll0876*
7	17.61	*slr0083*	7	63.41	*sll0226*
8	18.76	*slr1271*	8	66.67	*slr0329*
9	20.06	*slr0477*	9	76.38	*slr0211*
10	20.19	*slr1390*	10	81.98	*slr0241*
11	25.88	*slr0240*	11	85.62	*slr1147*
12	26.13	*slr0476*	12	96.21	*slr2102*
13	26.35	*sll1028*	13	102.60	*slr1916*
14	28.17	*ssl1552*	14	112.15	*sml0002*
15	29.58	*slr0082*	15	116.36	*slr1042*
16	32.19	*sll0615*	16	127.71	*sll0615*
17	33.63	*sll1181*	17	131.19	*sll0148*
18	34.67	*slr1265*	18	132.45	*slr0959*
19	34.72	*slr0211*	19	135.70	*slr0612*
20	35.42	*sll0148*	20	137.91	*slr0212*
21	36.22	*sll1172*	21	141.83	*slr0088*
22	36.37	*slr1031*	22	148.97	*slr0249*
23	36.72	*slr0181*	23	168.13	*slr0477*
24	37.13	*sll0849*	24	169.04	*slr0650*
25	37.17	*sll0404*	25	176.36	*slr0640*
26	39.66	*sll1173*	26	187.12	*slr0645*
27	42.23	*slr0212*	27	197.07	*slr1677*
28	42.82	*slr0357*	28	210.75	*slr0324*
29	43.47	*ssr1736*	29	214.16	*slr1793*
30	45.90	*slr1882*	30	268.19	*slr0240*
⋮	⋮	⋮	⋮	⋮	⋮
60	92.50	*slr1138*			
⋮	⋮	⋮			
68	96.32	*sll1968*			
⋮	⋮	⋮			
253	173.15	*slr1136*			
⋮	⋮	⋮			
475	1687.94	*slr0249*			
⋮	⋮	⋮			

Table 2-3. Ranking of mutant-specific weighted dissimilarities of mutants to the *sll1961* mutant. ORF IDs of *pmgA* (*sll1968*) mutant and candidates for the photosystem stoichiometry mutnats obtained in chapter I are indicated in red. ORF IDs of the candidate for the photosystem stoichiometry mutnats obtained in this chapter are indicated in green.

	Low light			High light	
Rank order	Dissimilarity	ORF ID	Rank order	Dissimilarity	ORF ID
1	3.83	*slr0185*	1	0.09	*sll1968*
2	3.92	*slr1916*	2	0.20	*slr0172*
3	4.33	*slr1390*	3	5.09	*sll1028*
4	5.51	*slr0636*	4	5.86	*sml0002*
5	6.97	*slr0083*	5	6.74	*slr1136*
6	7.52	*slr0476*	6	6.90	*slr1138*
7	7.58	*slr0212*	7	7.49	*slr0959*
8	8.40	*sll0404*	8	9.35	*slr1916*
9	8.62	*slr0477*	9	9.85	*slr0329*
10	9.26	*sll1173*	10	10.69	*sll0615*
11	9.63	*sll0148*	11	12.20	*slr0249*
12	13.65	*slr0211*	12	14.70	*sll0876*
13	14.78	*sll1028*	13	15.60	*slr2102*
14	16.16	*slr1911*	14	23.11	*slr1147*
15	16.29	*ssr1736*	15	23.97	*sll0226*
16	17.28	*slr2023*	16	25.17	*slr0241*
17	18.16	*sll1143*	17	25.78	*slr0211*
18	18.69	*ssl1552*	18	29.67	*slr0324*
19	18.96	*sll0716*	19	33.05	*slr1677*
20	19.05	*slr1031*	20	36.56	*slr0212*
21	19.12	*slr0495*	21	39.29	*slr1793*
22	20.10	*slr0795*	22	42.97	*slr0650*
23	20.64	*sll1193*	23	43.05	*slr0477*
24	20.82	*slr1325*	24	46.31	*slr1042*
25	21.96	*slr1302*	25	46.83	*slr0088*
26	22.13	*slr0838*	26	50.33	*sll0148*
27	22.13	*slr0603*	27	59.78	*slr0612*
28	22.34	*slr0480*	28	66.28	*slr0640*
29	23.18	*sll0876*	29	74.42	*slr0645*
30	23.71	*slr0181*	30	98.11	*slr0257*
⋮	⋮	⋮	⋮	⋮	⋮
65	37.35	*sll1968*			
⋮	⋮	⋮			
113	48.03	*slr1138*			
⋮	⋮	⋮			
161	56.37	*slr1136*			
⋮	⋮	⋮			
231	70.04	*slr0645*			
⋮	⋮	⋮			
472	391.75	*slr0249*			
⋮	⋮	⋮			

FIGURES

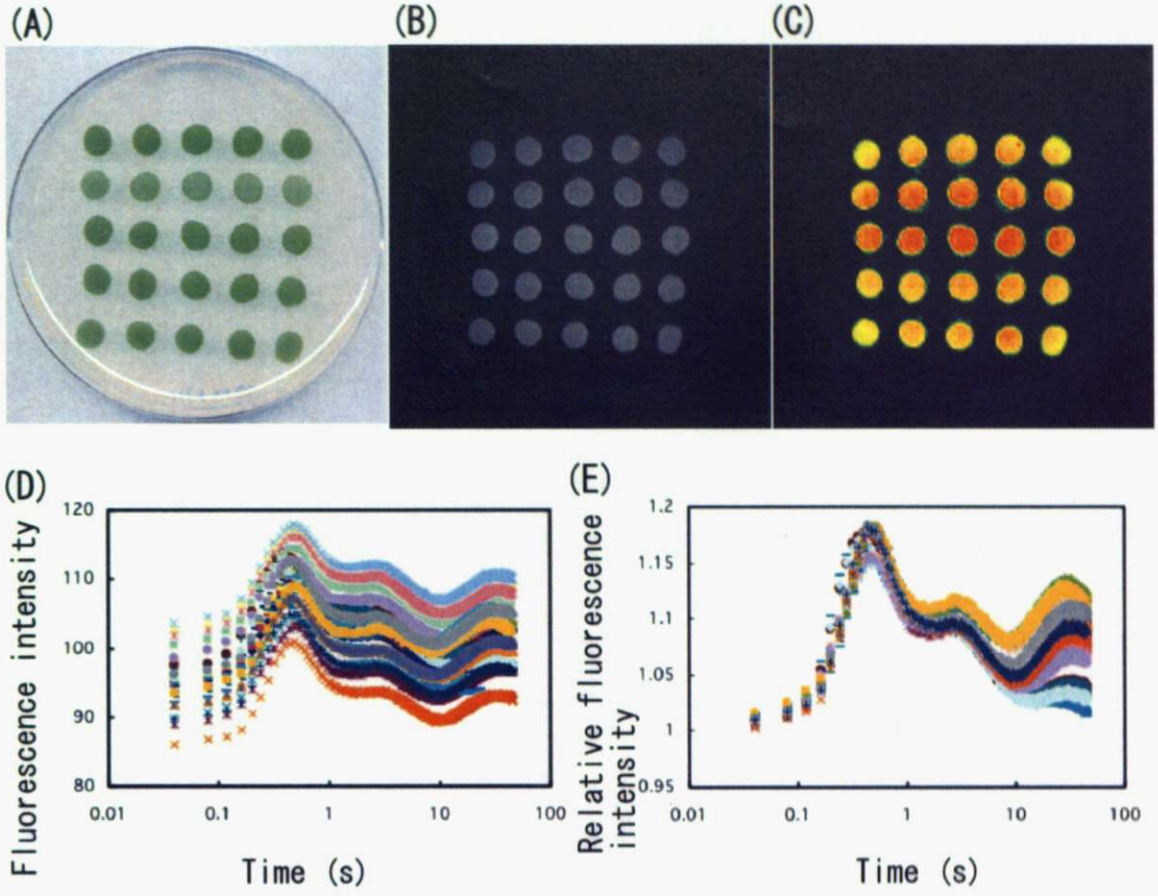

Fig. 1-1. Detection of chlorophyll fluorescence emitted from *Synechocystis* cells. 10 μl of cell culture, of which OD_{730} was adjusted to 0.5 by BG-11 liquid medium, was dropped on BG-11 agar plates. Cells of *Synechocystis* on agar plate were grown under high-light condition for 48 h (A). Scanning image of chlorophyll fluorescence in gray scale (B). Pseudocolor image of (B) (C). Chlorophyll fluorescence kinetics from each cyanobacterial patch (D). Normalized kinetics of (D) (E).

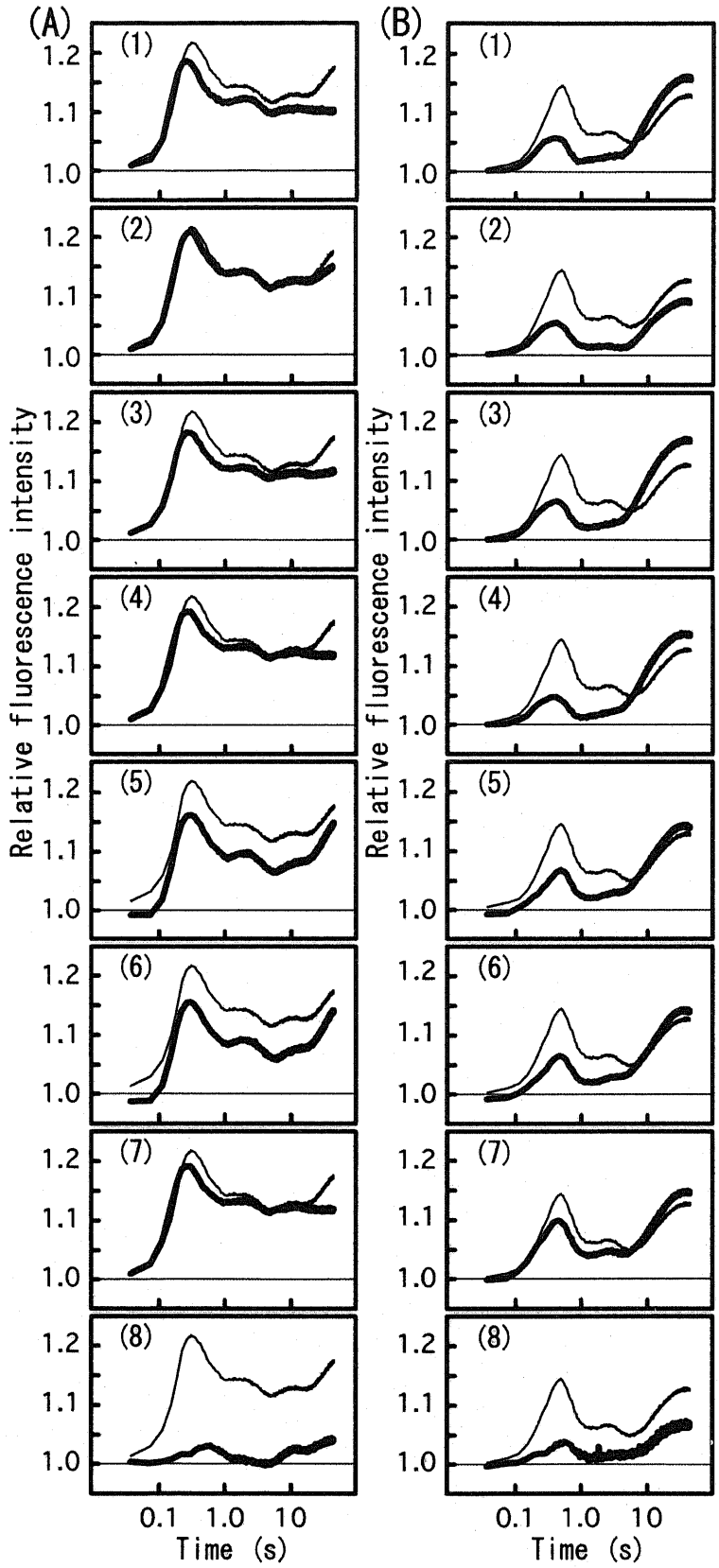
(A)
(B)
(1)
(2)
(3)
(4)
(5)
(6)
(7)
(8)
1.2
1.1
1.0
Relative fluorescence intensity
0.1 1.0 10
Time (s)

Fig. 1-2. Chlorophyll fluorescence kinetics of the wild type (thin line) and the mutants (bold line) mutants under low (A) and high (B) light conditions. Bold lines in (1), (2), (3), (4), (5), (6), (7) and (8) indicate the *sll1961*, *pmgA*, *ccmK2*, *slr1916*, *ctaEI*, *ctaCI*, *slr0645*, and *slr0249* mutant, respectively. The cells on BG-11 media were illuminated with light at 200 μmol m^{-2} s^{-1} for 45 s to monitor fluorescence kinetics after 15 min dark adaptation. Intensity of the fluorescence was normalized with the initial value at the start of actinic light.

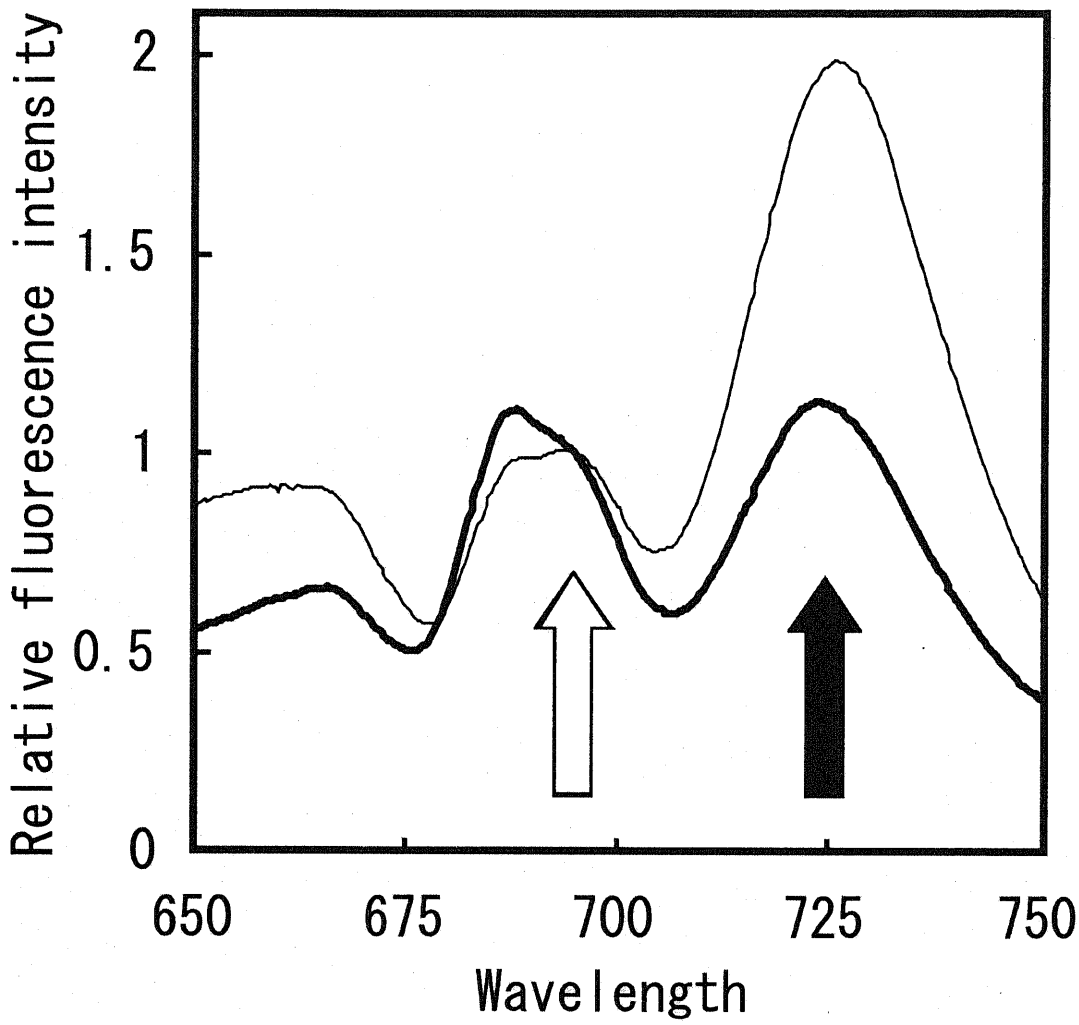

Fig. 1-3. Chlorophyll fluorescence emission spectra of low-light (thin line) and high-light (bold line) grown cells determined at liquid nitrogen temperature. White and black arrows indicate fluorescence peak of PSII (at 695 nm) and PSI (at 725 nm), respectively. The spectra were normalized by the fluorescence intensity at 695 nm.

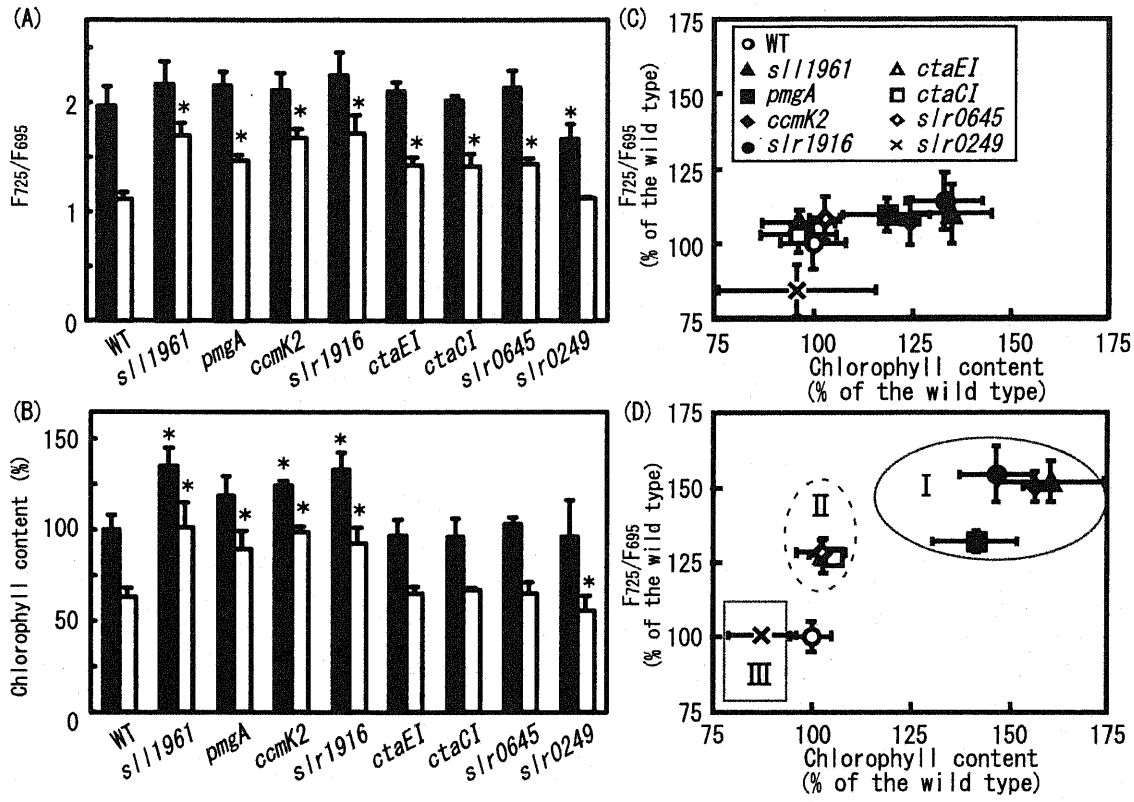

Fig. 1-4. Photosynthetic characteristics of the wild type and the mutants. (A) The ratio of F_{725}/F_{695} (PSII/PSI) and (B) the concentrations of chlorophyll in the wild type and the mutants. The wild type and the mutants were grown under low light (black bars) and high light (white bars) conditions for 24 h. The ratio of F_{725}/F_{695} was determined by measuring chlorophyll fluorescence emission spectra at liquid nitrogen temperature. The concentrations of chlorophyll were calculated by the equations of Arnon et al. (1974) from the absorption spectra of the cells. The chlorophyll contents were normalized at OD_{730} and expressed as a percentage of that for the low light grown wild type cells. Each value is the mean of three samples and error bars indicate SD. Asterisks indicate significant differences from wild type cells (Student's t-test; $P < 0.05$). (C), (D) Scatter diagram of the wild type and the mutants under low light (C) or high light (D) conditions with two parameters. The parameters are expressed as a percentage to the values of the wild type.

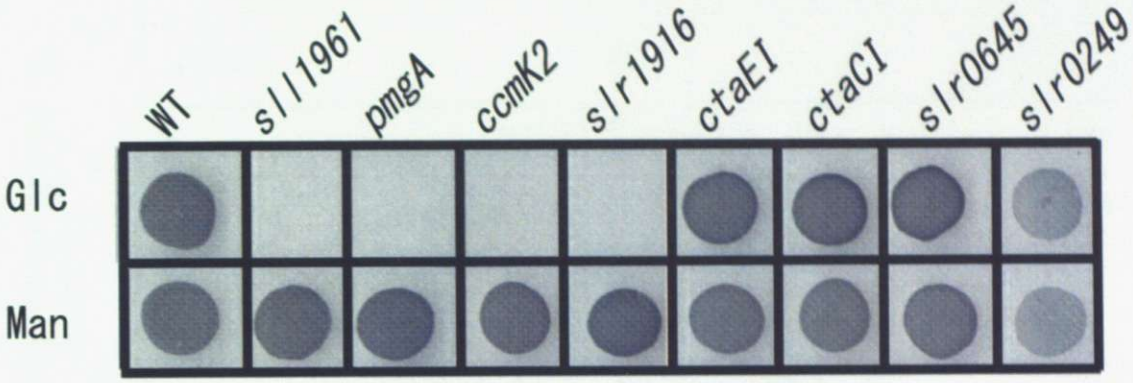

Fig. 1-5 Growth properties of the wild type and mutants under photomixotrophic condition. 10 μl of liquid cultured cells (OD_{730}= 0.5) grown under low-light condition were spotted on solid BG-11 medium. The cells were then grown for 3 days in the presence of 5 mM glucose (Glc) or 5 mM mannitol (Man) under medium light (100 μmol m^{-2} s^{-1}) condition.

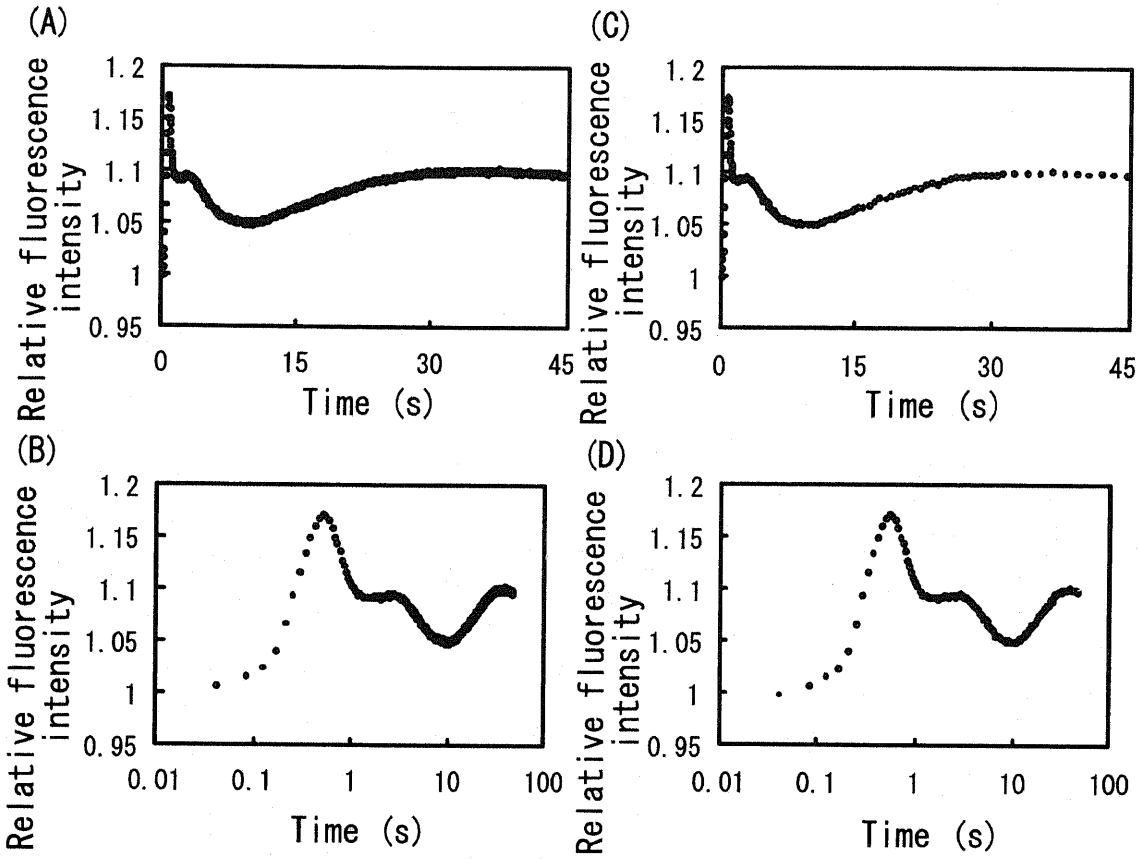

Fig. 2-1. Several different expressions of chlorophyll fluorescence kinetics emitted from the wild type cells. Time axis is in linear scale (A, C) or in logarithmic scale (B, D). The kinetic data are represented by all 1126 points (A, B) or by averaged 135 points (C, D).

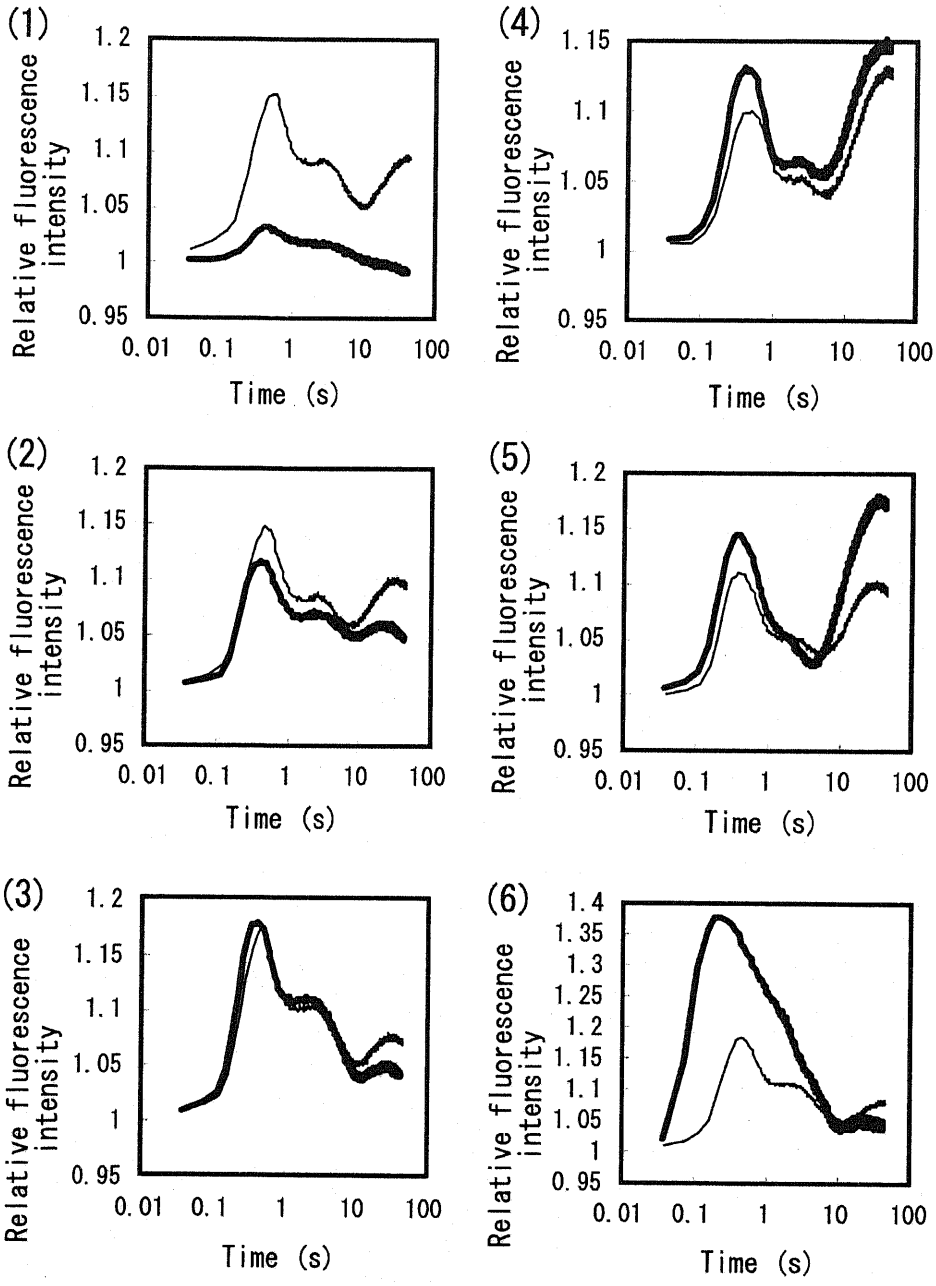

Fig. 2-2. Examples of a wide variety of fluorescence kinetics. The cells of the wild type (thin line) and the mutants (bold line) on BG-11 media were illuminated with light at 200 μmol m^{-2} s^{-1} for 45 s to monitor fluorescence kinetics after 15 min dark adaptation. Intensity of the fluorescence was normalized with the initial value at the start of actinic light. Bold lines in (1), (2), (3), (4), (5) and (6) indicate the *appC*, *pgt*, *pilC*, *ssl0352*, *glcE* and *ndhF1* mutant, respectively. Cells were grown under high-light condition.

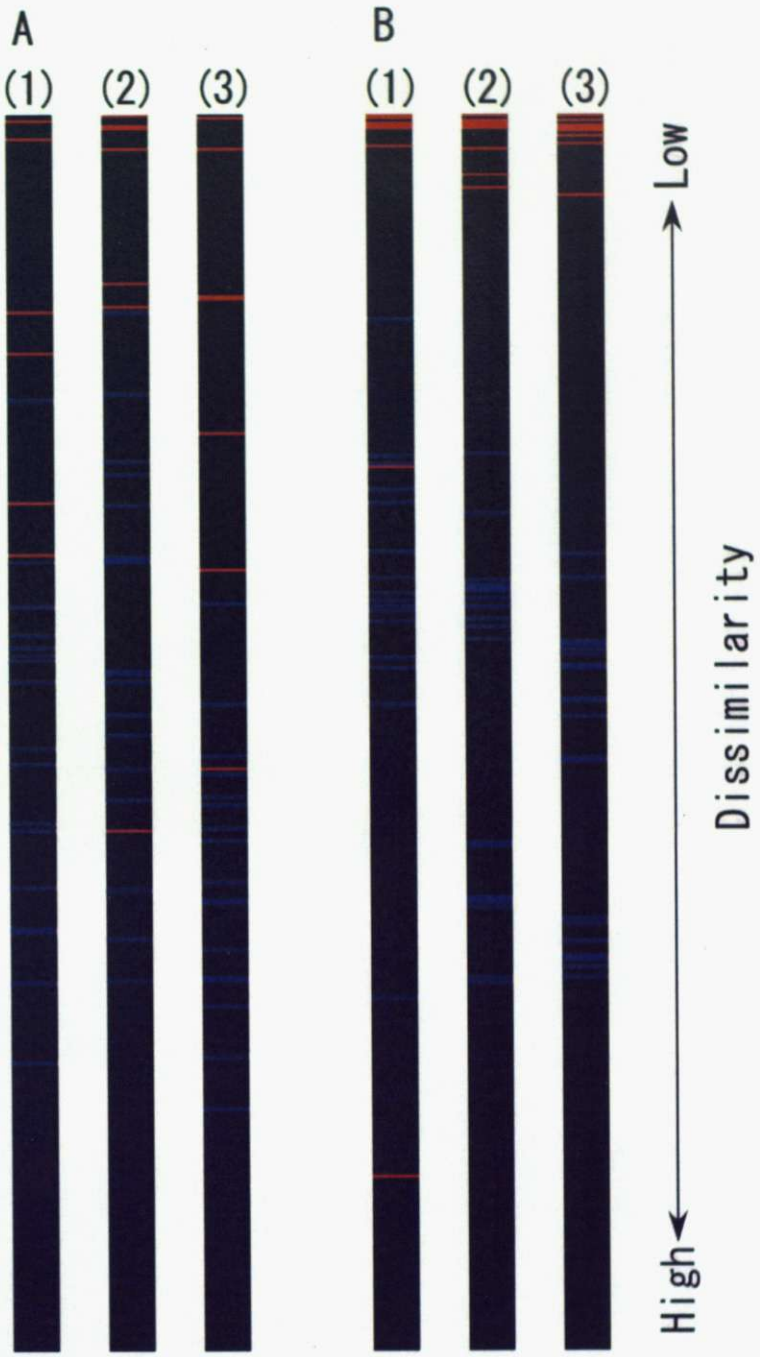

Fig. 2-3 Distribution of several strains in the ranking in simple (1), early-weighted (2) and mutant-specific weighted (3) dissimilarities. Cells were grown under low-light (A) or high-light (B) conditions. Dissimilarityes of *pmgA* mutant and candidates in chapter I are indicated in red. Dissimilarities of sixteen independently cultured wild type cells are indicated in blue.

(A)

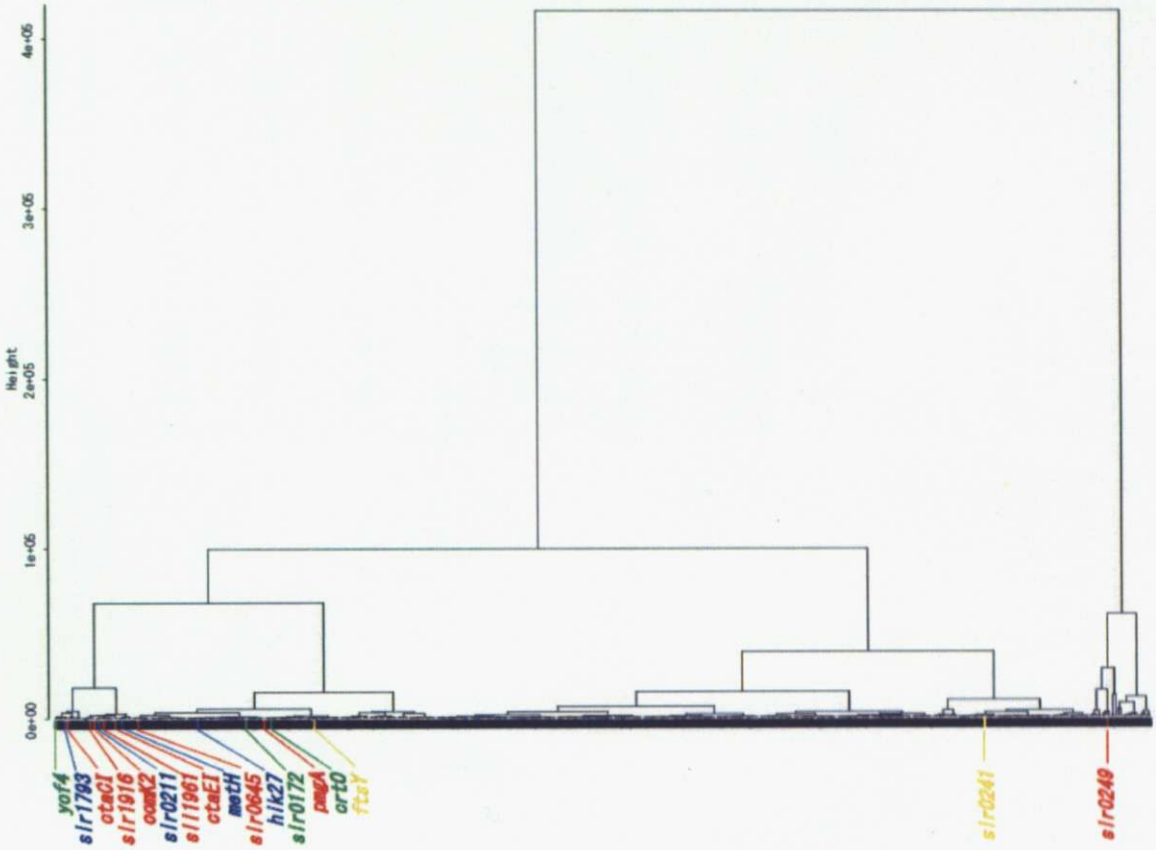
Height
0e+00
1e+05
2e+05
3e+05
4e+05
yof4
slr1783
ctaD1
slr1916
ocmK2
slr0211
sll1961
ctaE1
mctH
slr0645
hlk27
slr0172
pmjA
ort0
ftsY
slr0241
slr0249

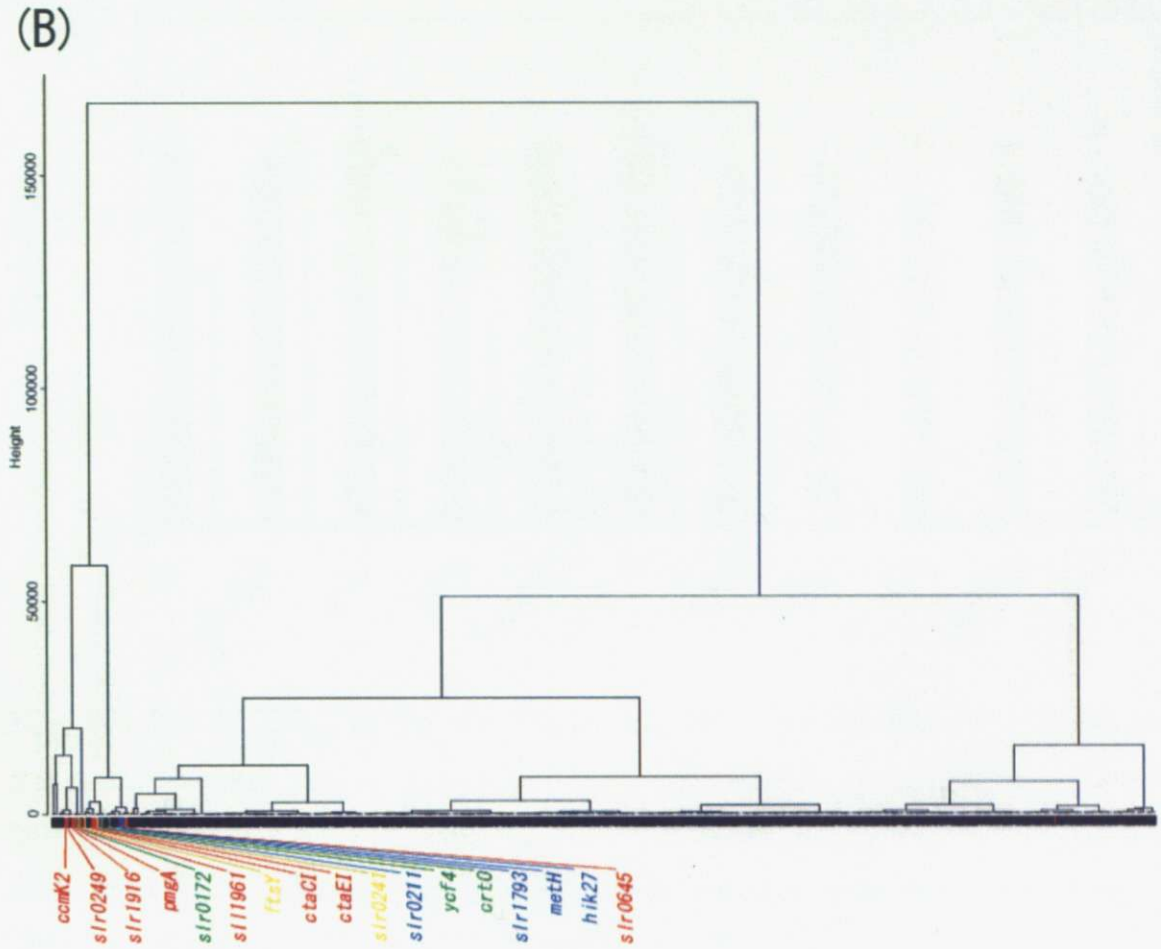

Fig. 2-4. Cluster analysis of the mutants based on the mutant-specific dissimilarity calculated for low- light (A) and high-light (B) grown cells. ORF IDs of *pmgA* mutant and candidates in chapter I are indicated in red. Green, blue and yellow indicate the candidates whom PSI/PSII ratio was determined. Green, blue, yellow indicate increased PSI/PSII ratio in high-light grown cells, normal PSI/PSII ratio in low-light grown cells, and dicreased PSI/PSII ratio in low-light grown cells, respectively.

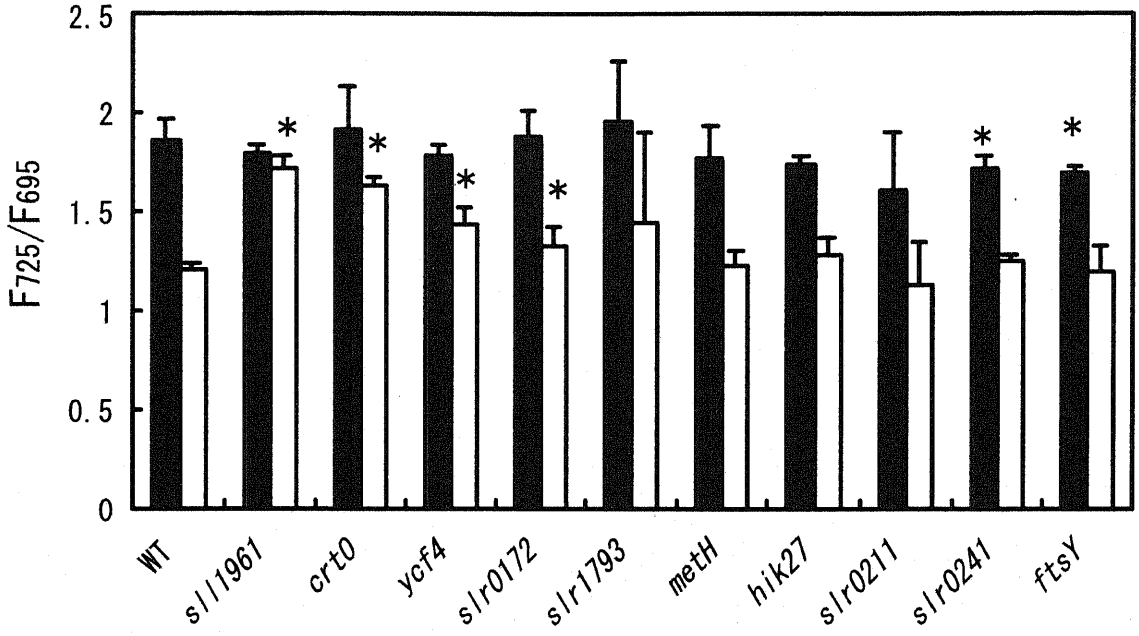

Fig. 2-5 The F_{725}/F_{695} in the wild type and the mutants. The wild type and the mutants were grown under low-light (black bars) and high-light (white bars) conditions for 24 h. Each value is the mean of three or four samples, and error bars indicate the SD. Asterisks indicate significant differences from the values of wild type (Student's t-test; $P<0.05$).

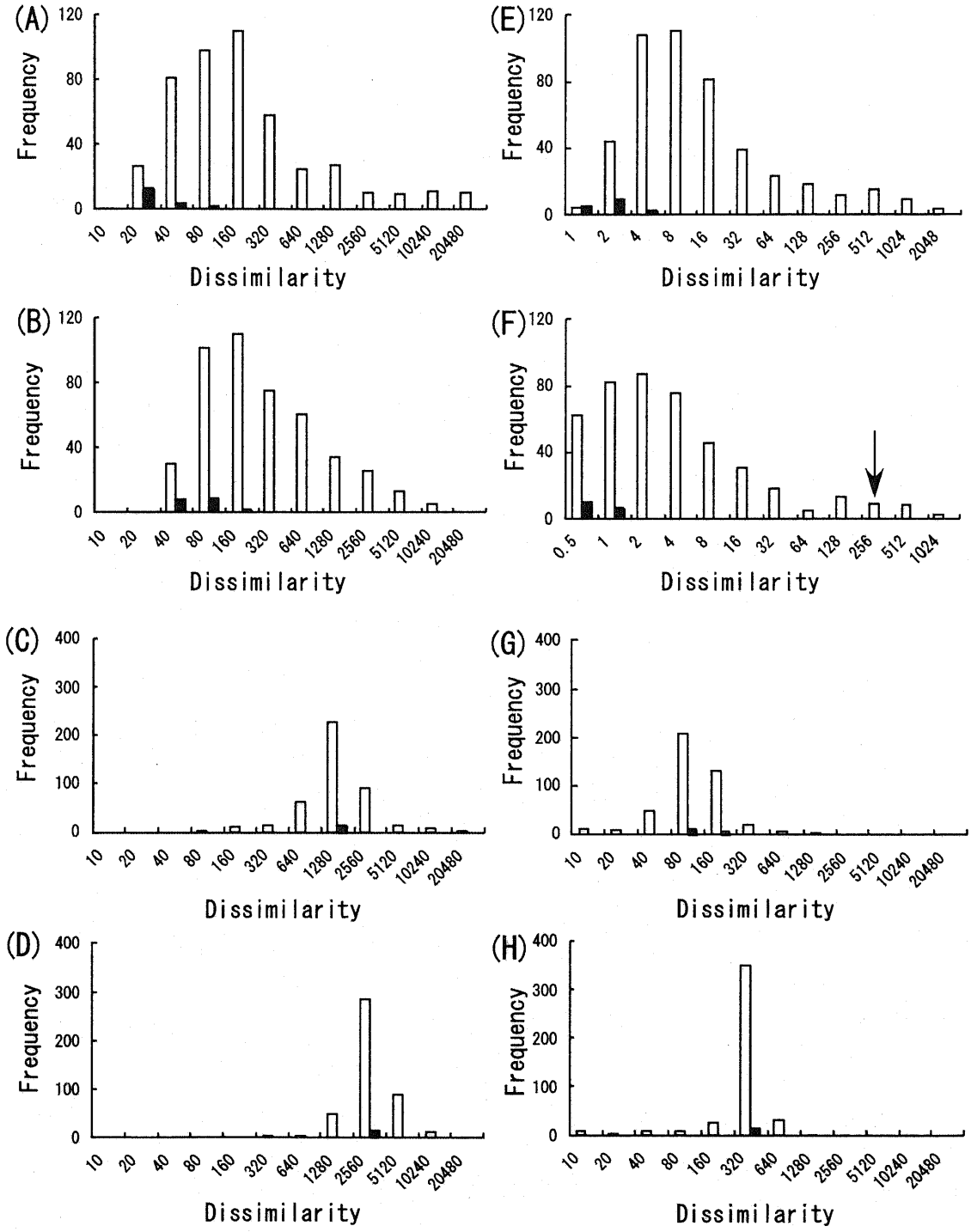
(A)
Frequency
120
80
40
0
10 20 40 80 160 320 640 1280 2560 5120 10240 20480
Dissimilarity
(E)
Frequency
120
80
40
0
1 2 4 8 16 32 64 128 256 512 1024 2048
Dissimilarity
(B)
Frequency
120
80
40
0
10 20 40 80 160 320 640 1280 2560 5120 10240 20480
Dissimilarity
(F)
Frequency
120
80
40
0
0.5 1 2 4 8 16 32 64 128 256 512 1024
Dissimilarity
(C)
Frequency
400
300
200
100
0
10 20 40 80 160 320 640 1280 2560 5120 10240 20480
Dissimilarity
(G)
Frequency
400
300
200
100
0
10 20 40 80 160 320 640 1280 2560 5120 10240 20480
Dissimilarity
(D)
Frequency
400
300
200
100
0
10 20 40 80 160 320 640 1280 2560 5120 10240 20480
Dissimilarity
(H)
Frequency
400
300
200
100
0
10 20 40 80 160 320 640 1280 2560 5120 10240 20480
Dissimilarity

Fig. 2-6.Frequency distribution of dissimilarities between the wild type and mutants (A, B, E, F) or between the *sll1961* and other mutants (C, D, G, H). Simple dissimilarities (A, B, C, D) and mutant-specific weighted dissimilarities (E, F, G, H) of the wild type (black bars) and the mutants (white bars) that were grown under low-light (A, C, E, G) or high-light (B, D, F, H) conditions for 24 h. An arrow indicates the value of dissimilarity of the *sll1961* mutant.

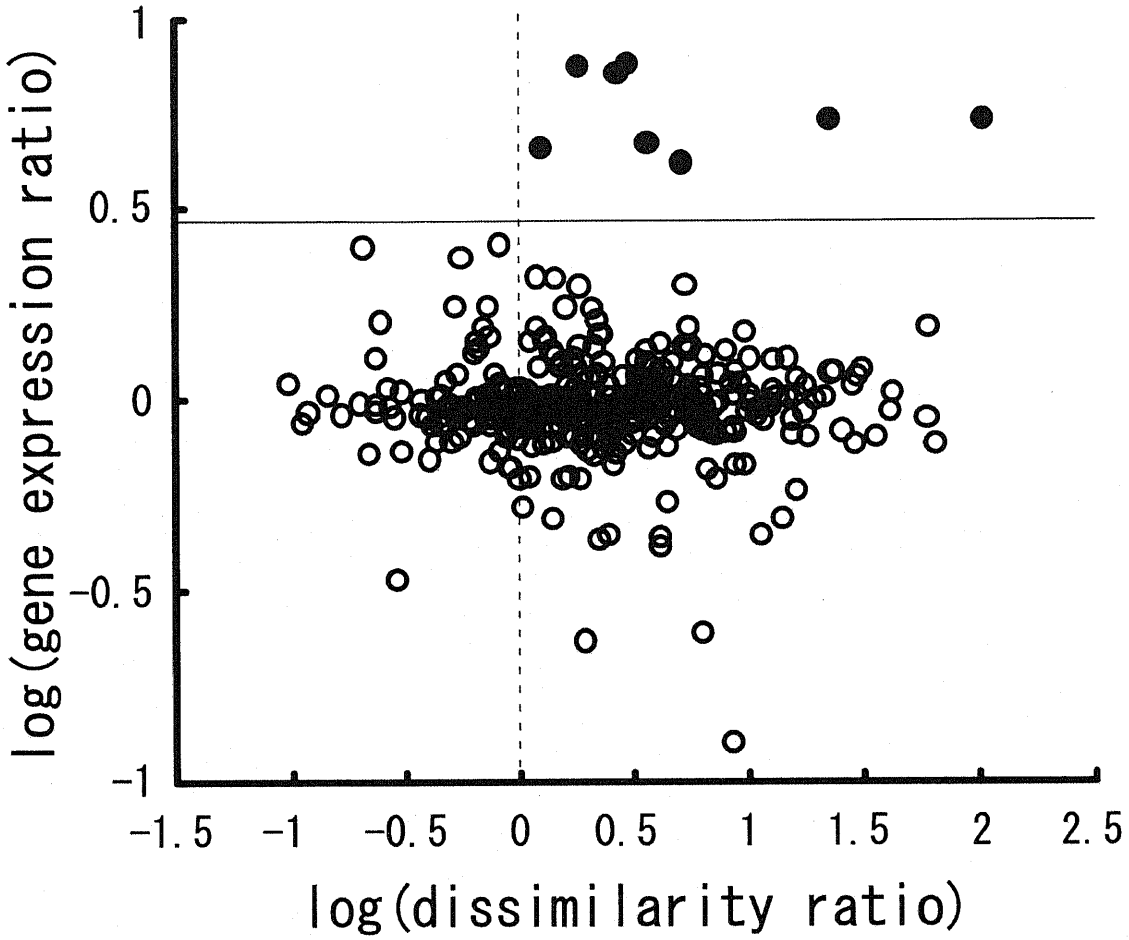

Fig. 2-7 Comparison of gene expression level and dissimilarity. The logarithm of the ratio of simple dissimilarity between the cells grown under high-light and low-light condition is plotted against logarithm of the expression ratio under high-light and low-light condition. Filled circles represent genes that showed significant increase in the gene expression under high-light condition.

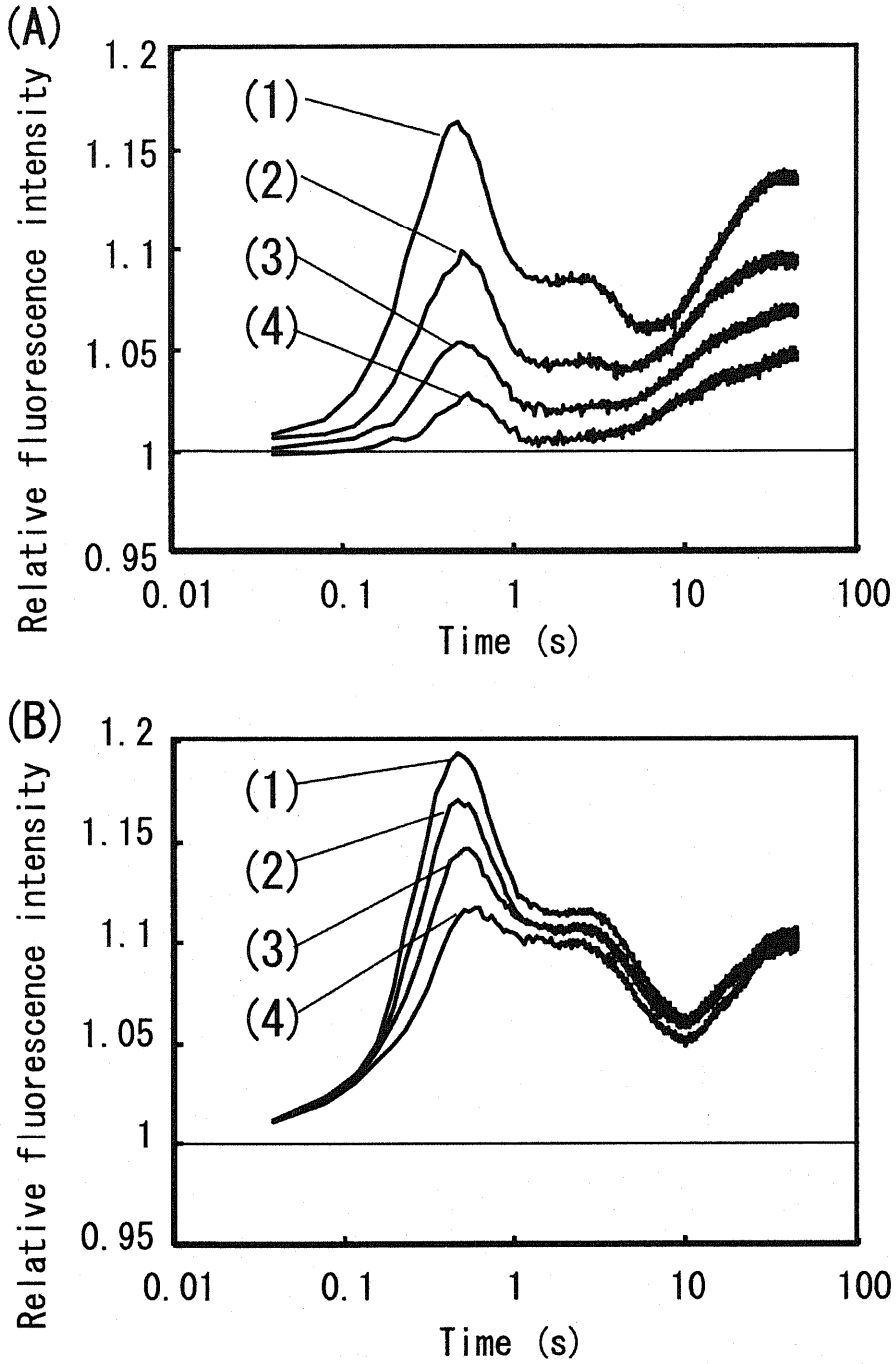

Fig. 2-8. Effect of photosynthetic inhibitors on chlorophyll fluorescence kinetics. The wild type cells were grown in high-light condition for 48 h on BG-11 plates and then 10 μl of 0 (1), 0.03 (2), 0.06 (3), 0.1 (4) μM DCMU solution (A) or 10 μl of 0 (1), 10 (2), 100 (3), 500 (4) μM MV solution (B) was dropped onto cyanobacterial patches on a plate just befor dark adaptation.